Characterization of Decellularized Porcine Tongue: A Matrix for 3D *in vitro* Head and Neck Cancer Models

Jacqueline Kort Mascort

B.BME., M.Eng Candidate

Bioengineering Department

Engineering Faculty
McGill University, Montreal
November 2018

Thesis supervisor: Joseph "Matt" Kinsella

A thesis submitted to McGill University in partial fulfillment of the requirements of the degree of Master on Engineering in Biological and Biomedical Engineering.

I. TABLE OF CONTENTS

II. LIST OF FIGURES AND TABLES

Figures

Tables

III. ABSTRACT

Squamous cancer of the head and neck (HNSCC) is the 6th leading cancer by incidence worldwide. It is associated with tobacco and alcohol use but can also occur by human papillomavirus (HPV). Efforts have been done to explain cancer progression, but understanding the significant interactions between the tumor, stromal cells, and the tumor microenvironment (TME) remains a challenge. Current methods of studying cancer biology in 2D yields limited insights into the physiological development of tumor tissues. On the other hand, traditional rodent models have many uncontrollable variables that result in biased conclusions. Therefore, we propose the creation of a matrix using decellularized extracellular matrix (dECM) for the fabrication of 3D *in vitro* models to study cancer. dECM has shown bioactive behavior promoting proliferation, differentiation, cell-ECM and cell-cell interactions. dECM active components make it an attractive bioink since, after decellularization, the material preserves several characteristics and components of the native tissue which cells recognize and react. In this project, we developed a method to decellularize and solubilize porcine tongue (dECMT). We determined the physical, chemical and biochemical characteristics, performed cell-viability assays and extruded the dECMT reinforced with Carbopol® ETD 2020NF using extrusion bioprinting. We suggest this material as the bioink to create 3D bioprinted *in vitro* models for mechanistic and translational studies for HNSCC.

IV. RÉSUMÉ

Le cancer malpighien de la tête et du cou (HNSCC) est le 6e cancer mondial par incidence. Il est associé à la consommation de tabac et d'alcool, mais peut également être associé au virus du papillome humain (HPV). Des efforts ont été faits pour expliquer la progression du cancer, mais la compréhension des interactions significatives entre la tumeur, les cellules stromales et le microenvironnement tumoral (TME) demeure un défi. Les méthodes actuelles d'étude de la biologie du cancer en 2D donnent peu d'indications sur le développement physiologique des tissus tumoraux. D'autre part, les organismes modèles traditionnels de rongeurs ont de nombreuses variables incontrôlables qui peuvent engendrer des conclusions biaisées. Ainsi, la création d'une matrice utilisant une matrice extracellulaire décellularisée (dECM) est proposée pour la fabrication de modèles 3D *in vitro* pour l'étude du cancer. dECM a démontré un comportement bioactif favorisant la prolifération, la différenciation, les interactions cellule-ECM et cellule-cellule. Les composants actifs de la dECM en font une bio-encre désirable puisque, après décellularisation, le matériau conserve plusieurs caractéristiques et composants du tissu naturel que les cellules reconnaissent et réagissent avec. Dans le cadre de ce projet, nous avons mis au point une méthode de décellularisation et de solubilisation de la matrice extracellulaire de la langue porcine (dECMT). Nous avons déterminé ses caractéristiques physiques, chimiques et biochimiques, effectué des tests de viabilité cellulaire et extrudé la dECMT renforcée avec du Carbopol® ETD 2020NF par bio-impression par extrusion. Nous suggérons l'utilisation de ce matériau comme l'encre biologique pour créer des modèles 3D bio-imprimés *in vitro* pour des études mécanistes et translationnelles pour le HNSCC.

V. ACKNOWLEDGEMENTS

First and foremost, I would like to thank my supervisor Joseph "Matt" Kinsella of Bioengineering Department at McGill University for his support and guidance through all this project. Coming to Canada, to his laboratory has been a great honor and a journey full of good experiences and learnings that made me grow personally and professionally.

I want to thank all the people that collaborated in this project: Dr. Simon Tran of Dentistry Department at McGill University and his students Osama ElKashty and Murali Ramamoorthi, without their suggestions and help in the biological interpretations of my project, the outcome would not have been the same.

Also, many thanks to Denis Flipo for his guidance in microscopy image acquisition, Dr. Kurt Dejgaard for his help with the manipulation and analysis of the proteomics presented in this project and Cleber Silveira Moraes for his help in sample preparation for histology and staining.

I would also like to thank funding agencies, CONACyT-i2t2, The Canadian Foundation for Innovation, Townshend-Lamarre Family Foundation, NSERC and McGill University for providing the financial support for me and this project.

Additionally, my laboratory co-workers and friends Miguel Alfaro, Salvador Flores Torres, Tao Jiang, Pooja Pushparaj and Jose Gil Munguia Lopez. Their positivity, capability to work as a team and willingness to share knowledge is invaluable, and I am incredibly grateful.

Finally, I would like to thank God for giving me the possibility to enjoy and learn from this experience and my family for their constant support even though I am far from home.

Author's contribution: All the work performed in this investigation including the experiments and the writing of the thesis were performed by Ms. Jacqueline Kort Mascort. Dr. Osama ElKashty did a pathological assessment of the dECM culture slices.

1. INTRODUCTION

Cancer is the second leading cause of death in developing countries, and the first cause of death in developed countries [1]. Squamous cancer of the head and neck (HNSCC) is the 6th leading cancer by incidence worldwide. In 2012, HNSCC accounted for 37% of the Human Papilloma Virus (HPV)-associated cancers in Canada [2], having 4.5 times higher incidence in males than females. To treat this disease, surgery, chemotherapy, and radiotherapy are successfully used in patients, but results in extensive damage to adjacent healthy tissues like salivary glands, leading to significant impact on the patients' quality of life [3]. Efforts have been made to understand HNSCC development and progression, but the constant change in the tumor microenvironment (TME), and the molecular mechanism associated with metastatic behavior post-treatment are not fully understood; resulting in up to 50% cancer relapse after two years of treatment when detected at a late stage. Conventional tools to study cancer biology including 2D cell monocultures and rodent preclinical models have been proven to be an important, but inadequate resource for they yield to limited insights. Alternative tools such as tissue engineered in-vitro tumor models have recently been developed including hydrogel 3D culture systems. Naturally-derived hydrogels such as decellularized extracellular matrix (dECM) have shown better performance in cell assays promoting cell adhesion, proliferation, and differentiation. This can be attributed to the presence of structural proteins such as collagen, glycosaminoglycans (GAGs) and insoluble factors [4, 5]. Hence, attempts to create *in vitro* models using bioprinting techniques for tissue engineering purposes have been previously reported [6-11]. However, there is a lack of research in the possible applications of dECM as a matrix for 3D *in vitro* cancer models.

We hypothesize dECM hydrogels obtained from porcine tongue (dECMT) can be used as a matrix to develop 3D bioprinted models of head and neck squamous cell carcinoma (HNSCC). In this

project, we decellularized and solubilized porcine tongue tissue for further physical and rheological characterization to determine its printability and propose reinforcement materials to improve matrix stability. Also, we characterized the biochemical composition and determined the viability of head and neck cancer cell lines (UM-SCC-12, UM-SCC-38) while encapsulated in dECMT.

The incorporation of dECMT reinforced with Carbopol® ETD 2020NF, a commercially available inert rheological thickener, into an *in vitro* model will use the bioactivity and biomimetic characteristics of the dECMT and the mechanical stability of Carbopol® ETD 2020NF. dECM will promote cell-cell and cell-ECM interactions for the biochemical and physical properties retained after decellularization and solubilization. The development of this model will minimize the gap between traditionally used 2D monolayer cultures and rodent models with the capability of controlling individual variables which are difficult to modify in animal models. This tissue engineering approach of preclinical models will offer a platform to understand the biology and progression of HNSCC in 3D and the controlled research for drug discovery with a tool that resembles the environment found in native tumrs *in vivo*. This technology is tissue-specific and can be adapted to study other neoplasms and diseases resulting in clinically relevant data that will potentially improve the treatment and prognosis of patients with HNSCC.

2. LITERATURE REVIEW

2.1.Head and Neck Squamous Cell Carcinoma (HNSCC)

Cancer [12] is defined as the abnormal and unregulated proliferation of cells that tend to invade normal tissues and organs spreading throughout the body. HNSCC is a group of biologically aggressive cancers that start forming in the epithelial cells of the mucosa found in the head and neck regions which include: salivary glands, nasal and oral cavity, paranasal sinuses, larynx and pharynx [13]. It is an illness that frequently metastasizes to the closely located bony structures in the head like the mandible, skull and lymph nodes [14] causing fast tumor spreading. Most of HNSCC cases including oral cavity cancers (OCC) and oropharyngeal cancers (OPC) are attributed to smoking and alcohol consumption [15]. However, the presence of Human Papilloma Virus (HPV) has also been an etiologic factor for OPC development.

Over the past decades, OCC incidence has decreased in developing countries [16] but OPC, which is associated with the presence of HPV, has increased in developed countries like Canada [17], United States [18] and United Kingdom [19] with a men-predominating population [20].

The standard of care for HNSCC includes surgery, radiotherapy, and chemotherapy [13]. These are commonly used together for advanced-stage cancers, but the treatment is highly dependent on the site of the primary tumor [13]. Treatments may result in malformations after surgical interventions, secondary cancer development due to radiation, mucositis, dermatitis, myelosuppression [21] and an overall decrease in patient's quality of life. Up to 50% of advanced HNSCC tumors recur after treatment with limited options of reirradiation or secondary surgeries [21]. In some cases, chemotherapy may be used after relapse with only 10–35% of response and less than a year of survival [22]. To improve the prognosis in HNSCC patients, new targeted therapeutic strategies are being developed, but the constant change in the tumor microenvironment

(TME), and the molecular mechanism associated with metastatic behavior post-treatment are not fully understood, together with the lack of translatable and predictive preclinical models of the disease, drug development becomes slower and more difficult.

2.2.The Tumor Microenvironment

TME is a complex arrangement of cells, structures, and molecules [23] that give tumors their distinctive architecture and behavior, enhancing the growth of the primary tumor and promoting metastasis to distant organs. Primary tumors are composed of a core of tumor cells surrounded by stromal cells (Figure 1), among the most common cell types found in the TME are [23]:

- Vascular endothelial cells, they form vessels to provide nutrients and oxygen to the tumor and a site for metastasis. Their formation is triggered by the angiogenic factors secreted by malignant cells. Vessels are supported in the periphery by the pericytes [23].
- Lymphatic endothelial cells, they are crucial for the dissemination of cancerous cells through the lymphatic system, their proliferation is highly dependent on VEGFC or VEGFD secretion factors [23].
- T lymphocytes, they are immune cells with phenotypes that can inhibit or promote tumor formation, their state is variable and dependent on the type of cancer [23].
- Myeloid cells, include tumor-associated macrophages (TAMs), myeloid-derived suppressor cells (MDSCs), Tumor-associated neutrophils (TANs) and terminally-differentiated myeloid dendritic cells [23]. This group is the most abundant cells found in TME, and their activities are usually pro-tumorigenic [24].
- Mesenchymal stem cells (MSC), they are recruited by the malignant cells to give rise to cancer-associated fibroblasts (CAFs), pericytes, adipocytes, and smooth muscle. CAFs are

found in many human and experimental cancers; they produce tumor-promoting chemokines, cytokines, growth factors, ECM components and enzymes that change the ECM structure [23].

Another component that plays a vital role during tumor progression is the extracellular matrix (ECM). The ECM is a collection of different components such as proteins, glycoproteins, proteoglycans, and polysaccharides. ECM composition is tissue dependent, and its properties are essential for cell regulation. It serves as a cell scaffold which allows cell-sensing and interaction with their environment from the surface of the cell to the nucleus, promoting changes in gene expression and cell behavior dependent on the environment. ECM can initiate signaling and has a regulatory feedback mechanism with the cells that allows tissue adaptation to their environment [25]. It has physical, biochemical and biomechanical properties that in cancer become deregulated and disorganized. Anomalous ECM deeply impacts cell migration out of the TME, facilitating metastasis and inflammation [26].

Abnormal ECM contains growth factors such as chemokines and angiogenic factors secreted by the stroma that interact with cell receptors, triggering pro-tumor pathways and modifying the tissue mechanical properties. The ECM is continually being remodeled by stromal cells' secretion of compounds, such as lysyl oxidase (LOX), which crosslinks structural proteins stiffening the environment, or degrading enzymes, such as collagenases, that soften the ECM promoting malignant cell migration. Increased deposition of naturally occurring structural proteins in ECM such as collagen, elastin, and fibronectin are commonly observed in native tumors [23, 27].

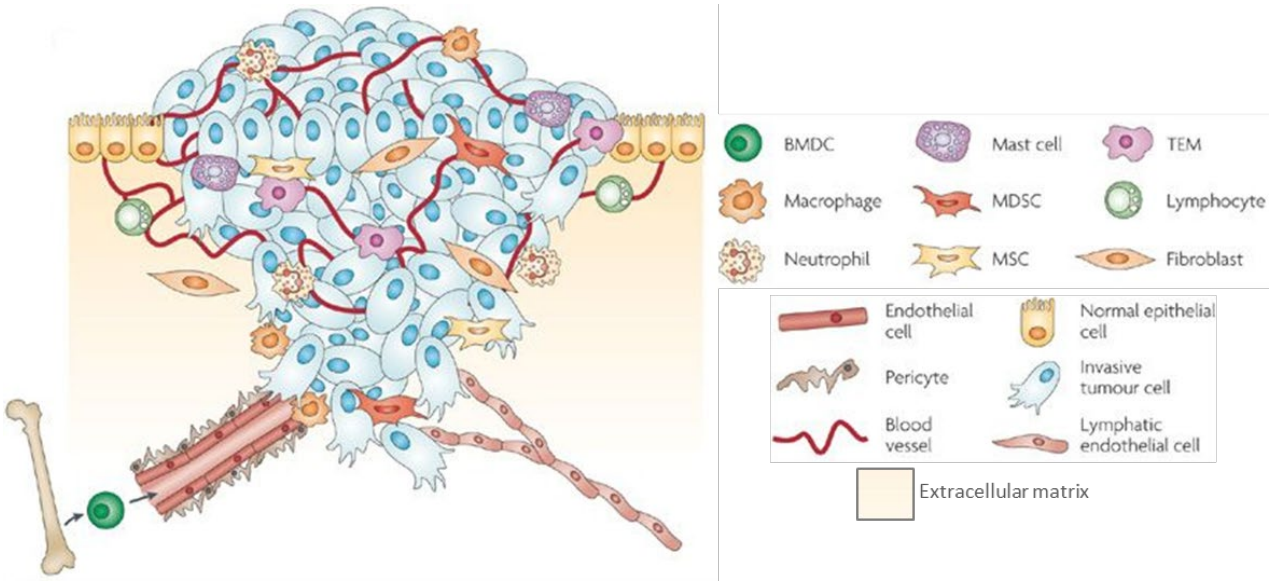

Figure 1- The tumor microenvironment:
Tumor cells are surrounded by different cell types including endothelial cells, several bone marrow-derived cells (BMSCs) including myeloid-derived suppressor cells (MDSCs), macrophages, TIE2-expressing monocytes (TEMs), mesenchymal stem cells (MSCs). TME has vascularization that supports tumor growth, and it is protected by the extracellular matrix which serves as a network for cues interacting and responding to stimuli of the TME [28]. Reprinted by permission from Springer Nature, Nature Reviews Cancer, Microenvironmental regulation and metastasis, Joyce & Pollard ®, 2008.

2D cell culture systems and rodent models have been extensively used in preclinical studies to study malignant neoplasms. However, literature studies have concluded that these models fail to recapitulate important characteristics of the disease present in the TME [29]. Currently, efforts and funding are directed towards designing physiologically-relevant models of study. Hence, we propose to engineer the TME by using native ECM materials mechanically reinforced with Carbopol® ETD 2020NF a commercially available inert rheological thickener. We expect our material to promote native tumor characteristics and drive intrinsic cell behavior while providing structure and support for cultured cells.

2.3.Traditional Pre-Clinical Models

Monolayer 2D cell culture is an important technique that has helped research evolve since the 1950s, and until today, it is the first step in understanding biological, chemical and molecular cues in living cells and drug discovery. This technique consists in growing cells on a hard substrate like plastic or glass, controlling the culturing conditions (temperature, CO_2, etc.) and keeping them alive with media supplemented with antibiotics, serum, glucose and specific chemical cocktails dependent on the cell requirements [30]. However, it is now recognized that 2D cultured cells are unable to exhibit the typical behavior and morphology [31, 32] found *in vivo*. Tissue-specific architecture, cell-cell, cell-ECM interactions, mechanical and biochemical cues are not present in this basic technique resulting in biased results [29]. Another used tool are animal models. These models provide additional information such as pharmacodynamic/pharmacokinetic (PD/PK) and pharmacological information which has been useful when identifying a target for disease treatment or discovering new therapeutic agents with rapid disease development [33]. Commonly used animal models for cancer, shown in Table 1, can help to obtain insights regarding cancer progression, but their complexity results in variables that are difficult to control such as tumor generation time, tumor size and area of development.

Additionally, the simplified scenario that immunocompromised rodents offer does not mimic physiological response, since the immune system is determinant in the evolution of neoplasms. Diseases as complex as cancer, which are continually changing are not well represented by these models. It is corroborated by nearly 7% of approval from pre-clinical discovery to phase I of clinical trials in oncology drugs, being the lowest among other types of drugs [34]. An alternative approach to improve pre-clinical cancer research and narrow the gap between 2D cultures and animal models, for failure determination at earlier stages of drug discovery, and understanding of

physiological processes, is the development of 3D *in vitro* cancer models. 3D models can be designed and tailored to accurately recapitulate the desired *in vivo* scenario and provide fundamental characteristics found in the TME [35].

Table 1- Traditionally Used Pre-Clinical Rodent Cancer Models

Pre-clinical cancer models	Description	Immuno-competence
Ectopic tumor xenografts using tumor lines [36].	Tumor cells or tissue is ectopically implanted in rodents to evaluate PD/PK and tumor growth or eradication after drug administration. They are useful to determine dosage and drug efficacy. Metastatic rates are low, it lacks TME.	IC, ID
Orthotopic tumor models using tumor lines [37, 38].	Tumor cells or tissue is implanted into the original tissue site of cancer to study. Fibroblasts, endothelial cells, inflammatory cells, and soluble factors are present and affect the tumor proliferation and development. Simulates TME better than the ectopic by having immunological and pathological responses resulting in higher metastatic rates. Reproducibility with this model can be challenging, and tumor heterogeneity is not present for working with established tumor lines.	IC, ID
Transgenic and genetically engineered mouse models (GEMMs) [39, 40]	GEMMs present mutations observed in specific cancers which promote tumor development spontaneously providing a TME without immunocompromising the animal. GEMMs have been useful to evaluate angiogenesis, metastasis and immune response. However, behaviors observed in this model may not be representative of tumor progression in humans, and the tumor formation in several sites interferes with the evaluation of the tissue of interest.	IC
Personalized tumorgrafts [41, 42]	Consist in the implantation of primary tumors into immunodeficient rodents preserving its genotypic and phenotypic features including heterogeneity and architecture.	ID

	These models have shown clinically relevant data, yet the implantation failure can be up to 30%. If successful they require from 6-8 months of propagation to be useful, therefore, the application to personalized medicine is limited.	
Carcinogen induced tumor models [43-46]	These models consist of the administration of tumor-promoting agents and are used to study the time-dependent and stage progression of cancer. The dosage and administration can modify the formation time and location of the consequent tumor. This model has been widely used to induce squamous cell carcinoma (SCC) in mice and hamster oral mucosa to evaluate the tobacco-associated development of SCC. The main weakness of these models is the long time required for tumor development that can be up to 50 weeks, resulting in high costs destined for animal care.	IC

IC: immunocompetent rodents; ID: immunodeficient rodents

2.4.3D *in vitro* Cancer Models

Different techniques have been developed to create 3D *in vitro* models. In this review, we are going to focus on organotypic explant cultures and multicellular spheroids [29].

The technique to create organotypic explant cultures consists in slicing the tissue of interest and culture it in a semi-porous membrane or a collagen gel. The advantage of this technique is the preservation of the structures and architecture found in tissue. This technique has been used for mechanistic studies in tissues with complex architecture like the brain [47]. The main issue of these cultures is the difficulty in imaging for the thickness and opacity of the sample. Also, modifications in the structure and controlled isolation of cells of interest is not possible (Figure 2A)

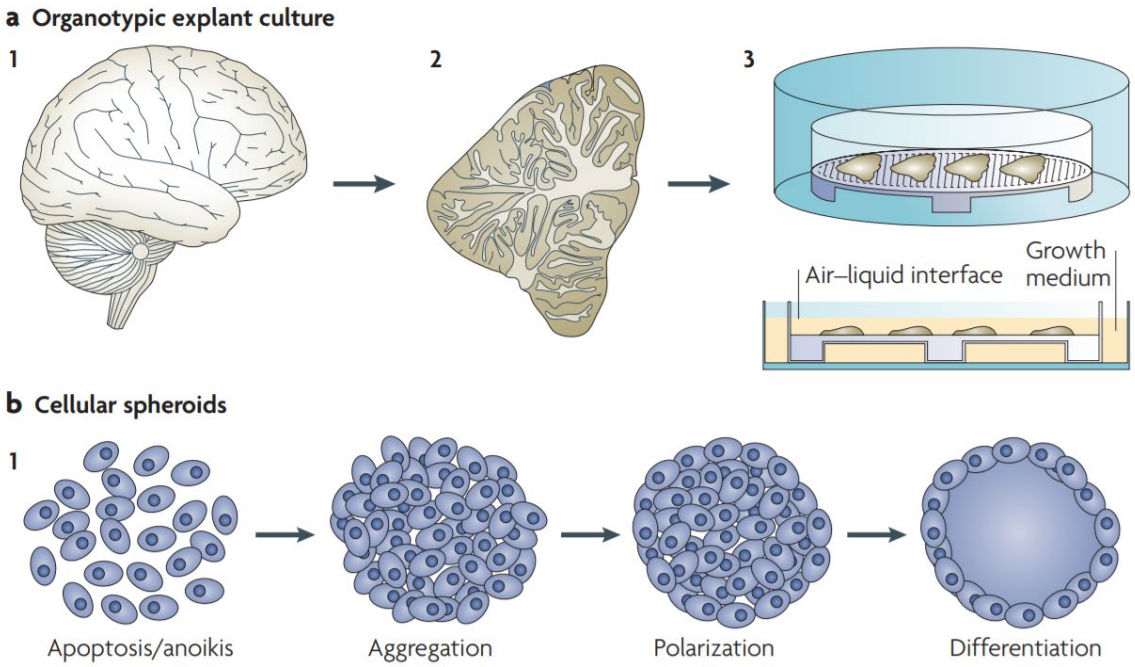

.

Figure 2- 3D Cell Culture Techniques:
A. Organotypic explant culture is produced by dissecting and slicing the organ of interest placing the tissue in a porous substrate and immersed in growth media. B. Cellular spheroids are formed by the cells' native adhesion behavior. When the cell aggregates into several hundreds of micrometers, they can differentiate into a hollow monolayer spheroid [29]. Reprinted by permission from Springer Nature, Nature Reviews Molecular Cell Biology, The third dimension bridges the gap between cell culture and live tissue, Pampaloni et. al ®, 2007.

On the other hand, tumor spheroids are structures formed by the cell's ability to aggregate. Single cell-type cultures and co-cultures have been reported. These spheroids may be produced using hanging drop [48] or rotating vessel techniques [49], are easy to model for their shape and can be incorporated into high-throughput drug screenings. The downside for cancer applications is the lack of ECM and the randomized position of cells when culturing multiple cell types (Figure 2B). To recapitulate the 3D environment *in vitro* is crucial to have a matrix that has similar mechanical properties that occur in healthy and/or anomalous tissue, with strategic cell positioning to mimic native structure. The matrix should be biomimetic and have accessibility to imaging tools which

are important for experimental development. Hence, additionally to our dECMT/Carbopol® ETD 2020NF bioink, we propose the use of extrusion bioprinting as an additive manufacturing technique due to its ability to form 3D constructs with desired architecture and dimensions.

2.4.1. Hydrogels as Extracellular Matrices

For our application, the biomaterial intended for 3D *in vitro* cancer models should be cytocompatible, bioactive to promote cellular anchorage and interaction with the matrix and be able to remodel according to the cellular secretion factors and organization. The mechanical characteristics should be similar to the tissue of origin and have porosity to promote waste-nutrient exchange. It needs to have mechanical stability and yield point high enough to prevent the collapse due to the force of gravity. Hydrogels, polymeric materials that maintain three-dimensional structure, are attractive for this cell culture application [50]. Their mechanical properties are in the range of most tissues in the body; they have networks that can hold a high percentage of water and biodegradable characteristics. Biocompatible hydrogels can be synthetic or naturally derived (Table 2).

Table 2- Representative Synthetic and Natural Hydrogels [50]

<table>
<tr><td colspan="3">Artificially Derived Gels and Hydrogels</td></tr>
<tr><td colspan="3">• PEG & derivatives
• Poloxamer (Pluronic ®)
• Poly (acrylic acid), (PAA)
• Laponite ®</td></tr>
<tr><td colspan="3">Naturally Derived Gel and Hydrogels</td></tr>
<tr><td>Polysaccharides</td><td>• Alginate
• Agarose
• Chitosan</td><td>• Pectin
• Cellulose
• Silk fibrils</td></tr>
<tr><td>ECM from mammals</td><td>• Gelatin
• Fibrin
• Hyaluronic Acid
• Collagen</td><td>• Matrigel ®
• Tissue-Derived Decellularized Extracellular Matrix Hydrogels</td></tr>
</table>

Synthetic materials such as Polyethylene glycol (PEG), Pluronic® and poly (acrylic acid) (PAA) can encapsulate cells and maintain them viable allowing cell deposition while they degrade [51]. However, the cultures result in low proliferation rate and low cell adhesion [52] for their lack of bioactive properties. Incorporation of peptides such as arginyl-glycyl-aspartic acid (RGD) can promote cellular binding to the matrix and higher proliferation rates [53]. Even though synthetic materials are controllable, reproducible and offer a consistent scaffold, the lack of bioactive components prevents cells from growing in their naturally occurring morphology and cannot sense endogenous factors that determine cell behavior [54].

On the other hand, natural materials are inherently biocompatible since they are derived from natural sources [50]. They can contain endogenous factors that promote viability, proliferation and development. However, modifying their mechanical properties may be challenging, and there is a risk of contamination during the preparation process. These scaffolds are complex, difficult to characterize and present batch-to-batch variability, but the biological significance is higher than synthetic materials [50]. For this project we are going to focus on mammal-derived materials:

Gelatin

Gelatin is partially denatured collagen from bovine or porcine skin that has naturally occurring RGD complexes. It is less immunogenic than collagen and a stable hydrogel at room temperature (20°C) but unstable at physiological temperature (37°C), although it can be crosslinked. It has been used in conjunction with chitosan and alginate to enhance mechanical properties and stability at 37°C. Alginate/gelatin composite encapsulated aortic root sinus smooth muscle cells (SMC) and aortic valve leaflet interstitial cells (VIC) which maintained viability over seven days of culture [55].

Fibrin

Fibrin is an insoluble protein formed by the reaction between thrombin and fibrinogen (both proteins involved in blood clotting mechanisms). It has shown the ability to support cell growth and proliferation [56]. It has non-linear elasticity properties [57] and a capacity to highly deform without breaking. It has been used to develop skin grafts and to co-culture human umbilical vein endothelial cells (HUVECs) with fibroblasts, resulting in angiogenic behavior [58]. However, fibrin degradation is so fast that makes it not compatible with long-term culturing. Also, it does not exhibit a shear-thinning behavior, the reason why it is not usually extruded. Additionally, the weak mechanical properties after gelation make the manipulation of fibrin challenging [59].

Hyaluronic acid

Hyaluronic acid (HA) is the simplest non-sulfated glycosaminoglycan (GAG) and is commonly found in most of the mammalian tissue. It is a linear polysaccharide composed of repeating disaccharides (β-D-glucuronic acid, N-acetyl-β-D-glucosamine) [60]. It plays an important role in wound healing, tumor development and inflammation [61]. To use HA as a hydrogel, chemical modifications to polymerize the molecule are needed to improve its rheological properties [62]. Also, the long gelation times promote cell sedimentation in 3D cultures resulting in a non-homogenous material. HA plays a vital role in embryonic development; hence it has been used to encapsulate human embryonic stem cells which maintain their phenotype and capability to differentiate [63]. HA has been combined with reinforcements like acrylated PEG and photo-crosslinked with UV irradiation [64] resulting in an extrudable material [65] capable of forming vessel-like structures.

Collagen

Collagen is the most abundant protein in mammalian tissue. There are almost twenty types of collagen, but the basal structure is composed of three polypeptide chains that form a triple helix structure held together by hydrogen and covalent bonds. Collagen's mechanical properties can be enhanced using chemical crosslinkers such as formaldehyde, genipin or glutaraldehyde. Physical crosslinking is also possible using heat or UV irradiation. Blends with natural [66] and synthetic [67] polymers have been reported. Collagen-alginate composites have show sustained viability of vocal fold fibroblasts over 42 days allowing ECM secretion. On the other hand, collagen-PEG hydrogels promoted cellular adhesion and proliferation of L929 fibroblast cells after seven days of culture with controlled degradation.

Decellularized Extracellular Matrices (dECM)

Decellularized extracellular matrices (dECM) are another family of naturally-derived biomaterials that is more complex than the materials mentioned above but has higher biological relevance. Decellularization is the process of removing cellular material from a culture, tissue or organ while keeping the structural and functional components of the ECM such as proteins (collagen, elastin, laminin, etc.), glycosaminoglycans, proteoglycans, and growth factors [68]. This process is a combination of mechanical, chemical and biologic agents (Table 3).

Table 3- Representative Decellularization Agents

Agent	Interaction with ECM	
Chemical Agents		
Triton X-100	Non-ionic detergent that mostly removes lipid-lipid, lipid-protein and DNA-protein interactions, and partially protein-protein interactions.	[69, 70]
Sodium dodecyl sulfate (SDS)	Ionic detergent that solubilizes cell and nuclear membranes. May denature and disrupt proteins.	[69, 71]

Acetone	Solvent that dehydrates the sample and removes lipids, it precipitates proteins.	[72, 73]
Biologic Agents		
Nucleases	Promote hydrolysis of DNA and RNA.	[70, 74]
Trypsin	Breaks peptide bonds between arginine and lysine from the C-side.	[71, 75]
Dispase	Breaks fibronectin and Collagen IV peptide bonds	[76, 77]
Physical Agents		
Temperature	Constant freezing and thawing forms ice crystals that disrupt the cell membrane but can affect the ECM stucture.	[78, 79]
Agitation/Perfusion	Helps with the removal of cell debris and promotes the contact of the tissue with the chemical and biological agents, aggressive agitation/perfusion may disrupt ECM.	[75, 80]

The origins of decellularization started with the isolation of basement membrane (BM). The basement membrane is specialized ECM that is more compact and less porous than the interstitial matrix, and it supports the structure in which epithelial and endothelial cells grow [81]. The main components of the basement membrane are collagen IV, heparan sulfate proteoglycan, laminins, growth factors, chemokines, cytokines and proteases [82]. In 1966, Bruchhausen & Merker isolated basement membrane (BM) components from rats' renal cortex by homogenizing the tissue and using a solution of 4% sodium deoxycholate to purify it from cell membrane fragments and debris. The contaminants were removed without disrupting the ultrastructure of the membrane. Clinical research in the 80's turned towards decellularization to preserve tissue for longer periods of time to use in wound dressing applications [83] or grafts. Today, we can find commercially available products harvested from porcine, bovine and human sources for clinical applications such as heart valves, dermis, intestine, pericardium [84], etc. Decellularization of whole organs is also possible by perfusion of decellularization agents through vasculature [84] while preserving the architecture of the whole organ. Successful decellularization of host cells and recellularization

of several organs such as heart [85], lung [74], liver [86] and kidney [87] has been reported. Tissues without vasculature like heart valves, skeletal muscle, trachea, etc. can be decellularized by immersion in decellularization agents and constant agitation until all cellular products are removed [84].

A famous landmark in 3D cell culture was introduced with the decellularization and isolation of basement membrane components from Engelbreth-Holm-Swarm (EHS) mouse sarcoma culture, now commercially available as Matrigel®. **Matrigel®** is a biomaterial stable at a physiological temperature which promotes proliferation and cell differentiation, although differentiation is dependant on the cell type. Endothelial cells in contact with Matrigel® showed attachment and alignment in one hour and formed vessel-like structures with a lumen in less than 24 hours [88]. It also promotes the generation of human-induced pluripotent stem cells derived from cardiomyocytes [89] and morphologies comparable to the tumor cells *in vivo* [90]. Even though Matrigel® components resemble the ECM environment of tissues, they should not be generally used for all application since every cell has specific ECM needs. The ECM found in bone, cartilage and breast tissues are significantly different in biochemical composition and mechanical properties. Also, chemokines, cytokines, growth factors and proteases present in Matrigel® could trigger different signaling and response on the encapsulated cells when comparing them to their behavior *in vivo*, since the source of the material is a secretion of a mouse sarcoma cell line [91].

On the other hand, dECM hydrogels derived from decellularized mammalian tissue, overcome the problem of having a dECM derived from sarcoma cells. The source of tissue to prepare dECM hydrogels generally corresponds to the cells of interest, after decellularization the insoluble components are solubilized using proteases and neutralized to obtain a stable hydrogel at physiological temperature and pH that supports 2D and 3D cell culture. There are three main tissue

solubilization methods: Voytik-Harbin [68], Freytes [92] and Uriel [93], for this project, Freytes method will be discussed.

In 2008, Donald O. Freytes from Badylak's group proposed a protocol to solubilize decellularized porcine urinary bladder and use it as a culturing biomaterial, which promoted the adherence and growth of rat aortic smooth muscle cells [92]. After decellularization, the dECM was solubilized using pepsin from porcine gastric mucosa in acidic conditions to cleave the non-helical bonds of collagen, destroying the triple helix structure [94]. Once the solution was neutralized, at temperatures above 22°C the collagen self-assembled by an entropy-driven process [94] and gelation occured (Figure 3). The biochemical composition depends on the native tissue but generally contains collagen I, sulfated glycosaminoglycans (sGAGs) and in fewer quantities collagen III, IV and VI. The presence of growth factors has also been confirmed in reduced amounts [4, 5].

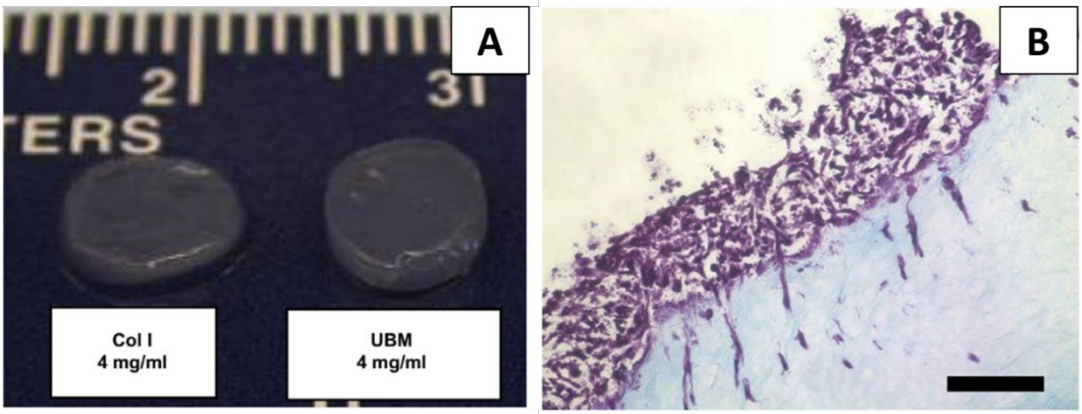

Figure 3- Freytes neutralized dECM
A. Freytes et al. neutralized dECM derived from porcine urinary bladder compared with Collagen I B at 37°C. Rat smooth muscle cells grown on UBM gels for ten days (scale bar = 100 mm) [92] Reprinted by permission from Elsevier, Biomaterials, Preparation and rheological characterization of a gel form of the porcine urinary bladder, Freytes et. al ®, 2008.

The viability of immortalized [95], primary [96] and stem cell [97] cultures in dECM hydrogels has been proven. Studies comparing Matrigel® and dECM hydrogels by culturing pre-adipocytes on the surface of both materials, confirm a better formation of colonies in dECM hydrogels after seven days of culture [93]. Human decellularized adipose tissue (hDAM) has been used as a matrix for a breast cancer model. Breast cancer cells 3D cultured in hDAM showed a different morphology, migration patterns, expression of adhesion molecules and sensitivity to drugs compared to Matrigel and 2D cultures [98]. Breast cancer cells grown in Matrigel formed spheres and islands while the ones grown in hDAM formed larger interconnected multicellular structures that were more than 1mm in diameter. The hDAM-cultured cells exhibited reduced sensitivity to doxorubicin, a chemotherapeutic agent commonly used in breast cancer treatment.

We recognize that native characteristics of tissue preserved after the dECM hydrogel preparation, are a resourceful and meaningful tool for studying malignant neoplasms *in vitro*. Hence, we chose porcine tongue as the proposed source material to develop *in vitro* cancer models of HNSCC. The rationale behind the source material selection is its proximity to the mucosa in the head and neck regions. Porcine species is considered for its success in clinical applications, the similarity with humans' physiological functions and known genomic profile [99]. Using bioprinting techniques to fabricate these models will take this model a step further by aiding in the positioning of specific cell types promoting the organization of the *in vitro* environment to resemble the TME.

2.5.dECM as a Bioink for Extrusion-Bioprinting

Extrusion bioprinting is a commonly used technique where syringe-like cartridges are filled with a bioprintable material (bioink) and pushed through a nozzle with a mechanical force or pneumatic

pressure into a flat stage. The cartridges can move in x, y and z directions following the instructions of computer-assisted design (CAD) files. The main advantages of extrusion bioprinting are:

- Manipulation of multiple cartridges permitting the use of different bioinks and cell types in the same design creating a heterogeneous model.
- The capability of heating and cooling the cartridges which is essential for temperature-dependant bioinks.
- Micrometer resolution is possible for the customizable nozzles that are commercially available.

[100, 101]

Efforts have been made trying to bioprint dECM bioinks using this method. Since the structure of the initial tissue is disrupted during the dECM hydrogel preparation, the mechanical properties of the final product are weaker. To compensate the weakness of dECM, the use of a polycaprolactone (PCL), a biocompatible and degradable polymer, has been reported as support for cell-laden dECM bioink of cartilage, heart and adipose tissue [102]. When tested for proliferation, these 3D constructs exhibited high cell viability and functionality, outperforming other bioinks such as collagen and alginate [102]. Photo-crosslinking of dECM has been attempted by using Vitamin B2 (Riboflavin) induced by UV light to enhance its mechanical stability. Cardiac progenitor cells were encapsulated in the Vitamin B2-containing dECM and bioprinted using extrusion-based techniques. The matrix was crosslinked while printing without affecting cell viability and proliferation [103].

Currently, research in dECM for bioprinting applications is shifted to the tissue regeneration and organ development *in vitro*. Findings from *in vitro* models can unravel essential aspects of cancer progression and treatment merging the complexity gap between traditional 2D cultures and

preclinical rodent models. For instance, in this project, the use of dECMT-Carbopol® ETD 2020NF bioink is proposed for 3D bioprinted *in vitro* cancer models. This biomaterial was developed by decellularizing porcine tongue and characterizing the mechanical, biochemical and cellular behavior of the dECMT to later incorporate Carbopol® ETD 2020NF.

Carbopol® ETD 2020NF is an tight coiled carbomer (Polyacrylic acid, PAA) interpolymer that contains a block copolymer of polyethylene glycol (PEG) and a long chain alkyl acid ester. that when dispersed in water, partially uncoils [104]. It has a cloudy appearance and a pH between 2.5 and 3.5 depending on the polymer concentration. When pH is adjusted between pH 6.5 and 7.5 maximum viscosity occurs because the acidic sections of the Carbopol® ETD 2020NF interact with the neutralizing base (such as sodium hydroxide, NaOH) creating a salt [104]. However, this thickening property decreases at pH 9 or higher due to the presence of excess electrolytes which affect electrostatic repulsion of the carboxylic groups of the PAA. Carbopol® ETD 2020NF acts as a rheological modifier at physiological pH and is commonly used in cosmetics and toothpastes to emulsify and thicken the consistency of the products [104]. In this project, after cr
ating different blends of dECMT and Carbopol® ETD 2020NF extrusion assays were performed to demonstrate the material's ability to be printed and incubated at physiological conditions while immersed in cell culture media.

3. MATERIALS AND METHODS

3.1.Decellularization of Porcine Tongue

Tongue decellularization was performed using the following protocol with some modifications [102, 104]. The porcine tongue was obtained from a local market. The mucosa was removed using a scalpel, cut into pieces of 0.5cm, ground using a food processor until the tissue was

homogeneously minced and weighted. Agitation in all the following solutions was 350RPM. A solution of 0.1% SDS (Bioshop®) in PB1X (Wisent®) and 1% Penicillin-Streptomycin (Wisent®) was used for 4 days changing the liquid every 24h using a strainer. The tissue was then stirred for 24h with PBS1X followed by a solution of 1% Triton X-100 (Bioshop®) for 24 hours. Then, a solution of DNAse (50u/ml) and RNAse (1u/ml) (Sigma Aldrich®) in dH_20 was used at 37°C for 4h. The sample was strained and incubated at 4°C in pure acetone (Sigma Aldrich®) overnight. The next day, the ECM was divided in 50ml centrifuge tubes and agitated with pure ice-cold acetone for 10 min to later centrifuge at 5000g for 10 min at 4°C, the supernatant was discarded from the tube. The last two steps were repeated 5 times to remove significant residues of SDS. After the final centrifugation, the samples were left open to air-dry at room temperature in a fume hood. To sterilize the dECM was stirred in a solution of 0.1% peracetic acid (Sigma Aldrich®) and 4% ethanol (Sigma Aldrich®) for 24 hours. All the following manipulations were performed under a biological safety cabinet to keep the dECM sterile. The peracetic solution was strained and washed with PBS 1X for 24 hours. Later, the tissue was strained and homogenized (Ultra Turrax TP-18 from IKA®) in PB1X with S25KG probe. Lastly, the sample was centrifuged at 5000g for 10 min and the supernatant removed. Samples were frozen at -80°C lyophilized and stored at -20°C.

3.2.Solubilization of dECM

To solubilize, Freytes [92] method was used with some modifications. For every 1 gr of lyophilized dECM, 200,000 units of pepsin from gastric mucosa (Sigma Aldrich®) were added to 100ml of 0.01M of HCl (Sigma Aldrich®), filter sterilized and stirred with the tissue at 350RPM until no pieces of dECM were visible (≈96h). Neutralization was completed keeping the dECM on ice and

adding 10ml of 0.1 NaOH (Sigma Aldrich®) (filter sterilized) and 11ml of sterile PBS10X (Wisent®) for every gram of lyophilized tissue. pH was adjusted to 7.4 using concentrated NaOH. Keeping the solubilized dECM at 4°C, it was filtered through a 100µm cell sieve centrifuging the sample at 5000g for 5 min at 4°C. The solubilized dECM was stored at -20°C prior to use.

3.3.Mechanical and Physical Characterization

3.3.1. Rheology

To characterize the mechanical properties of dECM and the reinforced blends, an oscillation rheometer MCR 302 (Anton Paar®) was used. A conical spindle with 25mm diameter and a cone angle of 1° (Part No. 79038). To determine the linear viscoelastic region of the dECM hydrogel, we ran an amplitude sweep test with a shear strain (γ) from 0.01% to 1000% at a frequency of 0.1H to obtain the linear viscoelastic region (LVR). Followed by a flow curve with a logarithmic ramp at a variable shear rate from 0.001 1/s to 1000 1/s. For the next experiments were performed using a 0.1% strain which is a value within the LVR in order to have a materials response independent of the magnitude of the deformation.

Then we performed a temperature ramp from 4°C to 37°C at 0.1% strain and at a rate of 0.2°C/min reaching a plateau at 37°C for 4 hours. 0.1% strain and 1Hz frequency were applied in this test for the results obtained in the amplitude sweep. All the experiments were performed in triplicate.

3.3.2. Scanning Electron Microscopy (SEM) Imaging

To visualize dECMT hydrogel internal structure, after stabilizing at 37°C the sample was fixed with 4% paraformaldehyde overnight and dehydrated up to 100% ethanol. Then, the sample was

immersed in liquid nitrogen and lyophilized. To acquire the data, SU-3500 SEM (Hitachi®) was used in variable pressure mode, 7kV, 60Pa up to 4,500x.

3.4. Biochemical Characterization

3.4.1. Liquid Chromatography-Tandem Mass Spectrometry (LC/MS/MS)

LC/MS/MS was used to determine the different proteins present in the dECMT. 1uL of dECMT was diluted into 10uL with 50 mM ammonium bicarbonate and added 1uL proteomics grade Trypsin (Promega®) to a concentration of 12 ng/uL. 1uL of this digest was injected onto a C18 trapping column (Acclaim PepMap 100, Thermo Scientific) and subjected to reverse phase LC-MSMS, using a nanoflow Easy-nLC 1000 UHPLC and a Q-Exactive HF Orbitrap mass spectrometer (Thermo Scientific®):

LC: Digest peptides were resolved on a 25 cm nano-Reverse Phase C18 UHPLC analytical column (Acclaim PepMap RSLC, Thermo Scientific®), running a water/acetonitrile (ACN) gradient from 3-20% ACN in 20 minutes and subsequent 20-35% ACN in the following 10 minutes (30 minutes in total) at a flow rate of 350 nL per minute.

MS: Eluting peptides were recorded by the Orbitrap mass spectrometer at a resolution of 120,000 and at a trap ion load of $3x10^6$. The top 25 most abundant ions at any given time point were subjected to isolation (isolation width: 2 m/z) and HCD fragmentation. MSMS spectra were recorded at a resolution of 15,000.

Data analysis: Acquired spectra (MS and MSMS) were extracted with Mascot Distiller (Matrix Sciences Ltd.) and searched again a relevant proteome database (Sus scrofa (Pig) - UniProt) using the 'Mascot' proteomics search engine (Matrix Sciences Ltd.) The searches were performed with the following settings: MS mass tolerance: 5 ppm. MSMS mass tolerance: 50 mDa. Digestion enzyme: Semi-trypsin. Missed cleavages: 2 Variable modifications: Methionine (oxidized).

Mascot search results were validated using the software analyses platform 'Scaffold' (Proteome Software Inc.), and identified proteins were visualized as total redundant spectral counts. This test was performed using triplicate samples of dECMT

3.4.2. Bradford Assay

To quantify total protein content, Bradford Assay (Biorad®) was performed using the protocol provided by the manufacturer using bovine serum albumin (BSA) for the control curve. One part of the concentrated dye reagent was diluted with 4 parts of distilled deionized water and filtered through a Whatman #1 filter. BSA standards were prepared from 0-300µg/ml. 10µL of the standards dilutions and dECMT were added to a 96-microtiter plate. Then, 100µL of the diluted Bradford reagent was added using a multichannel pipette and incubated at room temperature for 10 minutes. Absorbance was measured at 595nm using Nanodrop® 2000. The sample and standards were prepared in triplicates.

3.4.3. SDS Page

SDS-Page was performed to compare the proteins found in dECMT with commercially available Collagen I and determine if the α and β chains of dECMT collagen differed in molecular weight when compared to Collagen I. We used the protocol suggested by the manufacturer (Biorad®). Briefly, DTT was added to a concentration of 100mM to 2X Laemmli buffer to further mix at a 1:1 ratio with the dECMT in a 1.5ml tube. Tubes were heated at 95°C for 5 minutes. The Mini-PROTEAN® TGX® Precast gel was placed in the electrophoresis chamber immersed in running buffer. Samples and molecular marker were loaded and powered with 100V until all the lines of the molecular marker were visible in the gel. The gel was washed with deionized H_2O and stained with Coomassie Blue overnight. The next day the gel was immersed in a destaining solution (50%

dH_2O/ 40% methanol/ 10% acetic acid) with gentle agitation until the background was transparent and photographed for analysis. Triplicates of Collagen I and dECMT were evaluated in this assay.

3.5.Cell-viability assays

For all the cell viability assays mentioned below these two cell lines were used: **UM-SCC-12**, a moderately differentiated human squamous cell carcinoma immortalized cell line derived from the larynx of a male patient. **UM-SCC-38** a moderately differentiated human squamous cell carcinoma immortalized cell line derived from the tonsillar pillar of a male patient. Cell lines purchased from the University of Michigan.

3.5.1. 2D Cell Culture

To grow cells in 2D prior 3D culture, cells were cultured with DMEM supplemented with 10% Fetal Bovine Serum and 1% penicillin-streptomycin on T-flasks in a traditional incubator (5% CO_2, 95% humidity, 37°C). To passage the cells, trypsin-EDTA was used to disrupt cell attachments. All cell culture reagents were purchased from Wisent®.

3.5.2. Mold-casted 3D Culture

UM-SCC-12 and UM-SCC-38 were cultured in 2D until 80% confluence, trypsinized and counted. Cells were centrifuged, resuspended in less than 10µL and mixed with the solubilized tongue dECMT at a concentration of 500,000 cells/mL while keeping the dECMT between 4°C-10°C. 200 µL of cell-laden dECMT were added to a 48-well plate and placed in the incubator to allow dECMT gelation. Culture media was added on top of the dECMT after gelation. Discs were transferred to an agarose-coated dish for long-term culture after 24h.

3.5.3. Live-Dead Assay & Confocal Microscopy

3D cultured cell-laden dECMT were incubated in triple staining solution of Calcein-AM (Invitrogen®)/ Ethidium Homodimer (Invitrogen®)/ Hoechst 33342 (TOCRIS Bioscience®) to stain live, dead cells and nuclei respectively. To prepare the staining solution for 1ml of DPBS1X, 0.5µL of Calcein-AM (4mM), 2µL of Ethidium Homodimer (2mM) and 2.3 µL of Hoechst 33342 (18mM) were added. The tube was vortexed, and dECMT discs were incubated in the solution at 37°C for 30 minutes covered from the light. Before confocal imaging, discs were washed from the staining solution using PBS1X. The acquisition was made with Nikon A1+ confocal on random representative sites of the disc capturing the Z-stack (5 µM step size) of each point. Data analysis was done in Fiji® from ImageJ.

3.5.4. Histology

We did histology and used Haemotoxylin and Eosin (H&E) stain to observe cell morphology, cell arrangement and proteins present in the discs. The same samples used for confocal microscopy were fixed with ice-cold 4% paraformaldehyde overnight to follow a slow dehydration up to Ethanol 70%. After, full dehydration with ethanol 70%, 95%, and 100% was done with 1h incubation between each wash. Absolute ethanol wash was repeated three times, followed by another three 1h washes in xylene. Finally, samples were immersed in two wax baths of paraffin (1 hour per bath). 4mm sectioning and H&E staining (Leica ST Infinity H&E Stain) was performed using the Leica® TS5025 specimen stainer. Light microscopy images of these samples were acquired for pathological analysis. For these tests one disc per cell line per day was sliced 4 times with a thickness off 4µm and a step of 20µm between one slice and the other.

3.6.3D Bioprinting

Bioprinting of pure dECMT and dECMT-Carbopol® ETD 2020NF was performed using the Bioscaffolder 3.1 (GeSiM®). To print pure dECMT hydrogel the extrusion-based bioprinter has heatable cartridges which were set to 37°C to promote dECM gelation. $10cm^2$ cartridge was used with a conical tip (internal diameter: 25mm). Pressure requirements for extrusion varied between 30-45kPa following a square design of multiple layers and gridded pattern. For Carbopol® ETD 2020 NF solutions, the powder was mixed overnight with ddH_20 and pH adjusted to 7.4 with NaOH to further mix at different concentrations of the dECMT hydrogel.

4. RESULTS AND DISCUSSION

4.1.Decellularization and Solubilization

We were successfully able to decellularize porcine tongue following a combination of physical, chemical and enzymatic processes (Figure 4A-B). The acetone dilution of SDS was previously reported as a method to remove detergents when purifying a protein after SDS page [105] and we incorporated this step into our decellularization process with a successful outcome. The sterilization of the dECMT was performed using the 0.1% peracetic acid 4% ethanol solution resulting in a material that did not show bacterial formation after incubation at 37°C in LB media at 300RPM for 72h. The LB media was completely clear showing no signs of bacteria. The tissue was homogenized and solubilized using pepsin from porcine gastric mucosa (Figure 4C-D) obtaining a dECMT hydrogel which flows at 4°C and 20°C but maintains its shape when kept at 37°C (Figure 4E). dECMT, when mold casted in multi-well plates, keeps its shape and is easy to

manipulate with a spatula (Figure 4F). When dECMT does not contain cells, no apparent contraction occurs over long-term culture at 37°C. On the other hand, when cells are seeded, a contraction occurs over time [106] (Figure 4G). Gelled dECM does not dilute when immersed in media which is useful to keep the cells inside the matrix when culturing.

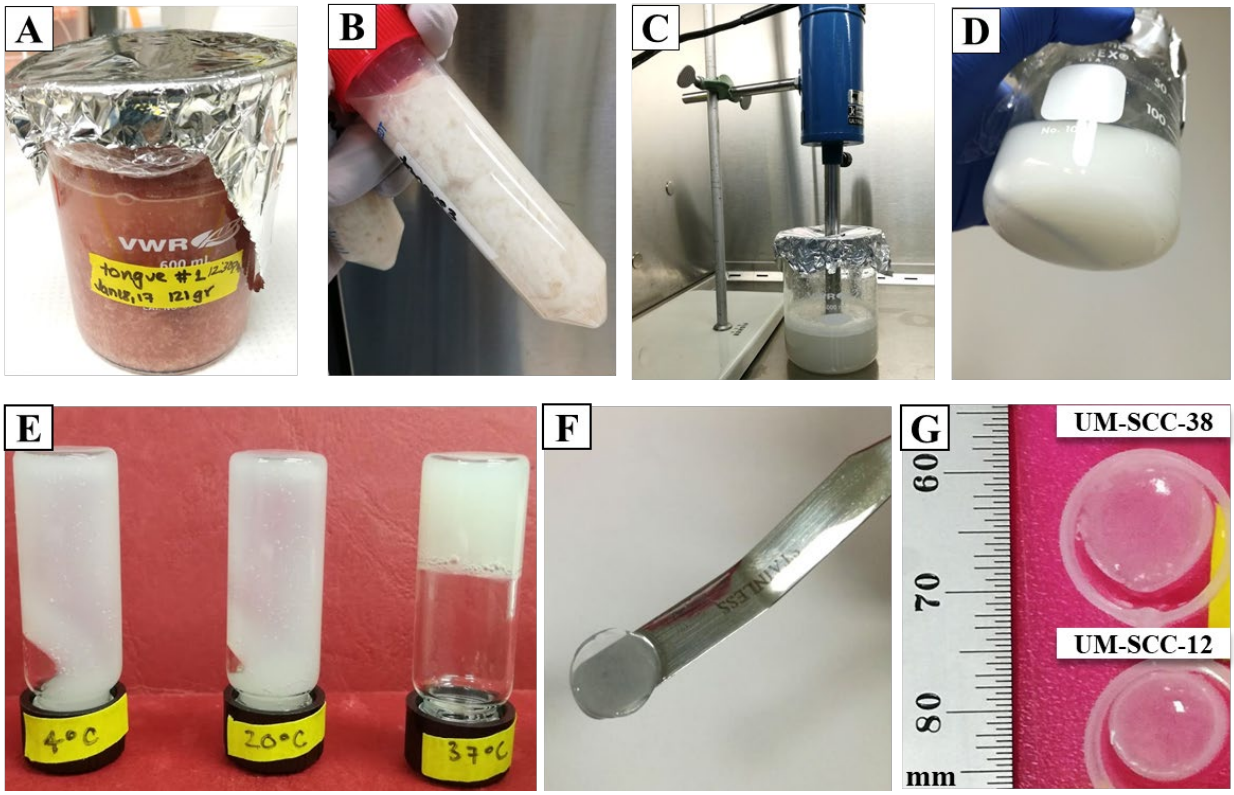

Figure 4- Decellularization and Solubilization Process:
A. Porcine tongue immersed in SDS solution. B. dECMT in pure acetone for detergent removal. C. Homogenization of dECMT in sterile conditions. D. dECMT solubilized with pepsin after 96h. E. dECMT after 24h of incubation at 4°C, 20°C and 37°C respectively. F. Mold casted dECMT manipulated with a spatula after 24 hours of incubation at 37°C. G. Mold casted cell-laden dECMT after 19 days of culture with UM-SCC-12 and UM-SCC-38 immortalized cell lines.

4.2.Physical and Mechanical Characterization

Rheological properties of the dECMT at pH 7.4 were measured (Figure 5A-C). Amplitude sweeps, and viscosity tests were done at 37°C which is the ideal temperature for printing and cell culturing. dECMT hydrogel shows an average storage modulus of 46.11Pa and a loss modulus of 8.58Pa in the linear viscoelastic region. The test was done after 2h incubation at 37°C. For all the tests performed later, a shear strain of 0.1% was used. A shear-thinning behavior is observed in the viscosity curve. Time sweep shows the change in moduli over time when the dECMT is at 37°C, the most abrupt change happens in the first 120 min reaching 89.45Pa after 180min. The temperature ramp shown in Figure 5D was done from 4°C to 37°C, a significant increase in the storage modulus is observed while the sample is at 37°C. The dECMT is always a gel independently of its temperature, this is observed in the rheology data which shows the storage modulus is always higher than the loss modulus. However, a higher difference between G' and G'' is observed at 37°C. SEM imaging was performed using variable pressure (VP) mode in the microscope since the material was not coated with a conductive layer. For that reason, high magnification images were difficult to acquire without damaging the sample, but AFM (Figure 5F) imaging confirms the presence of collagen. The displacement between one collagen molecule and another is 67nm of distance, when measuring the bands in the structure shown in Figure 5F the distance was 68.3nm [107].

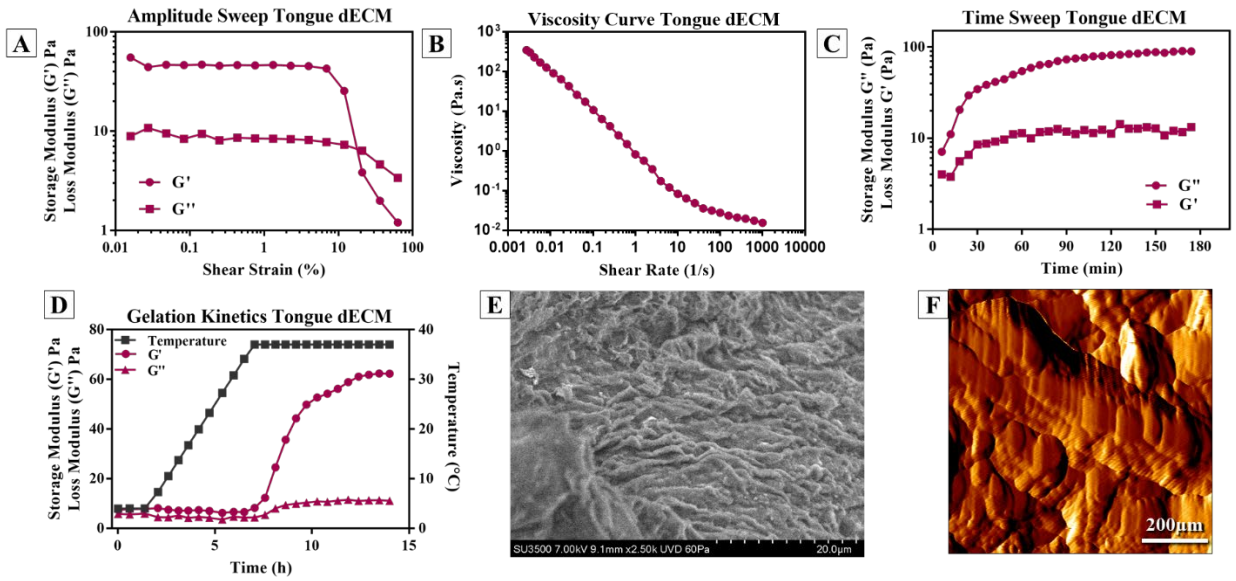

Figure 5- Physical and Mechanical Characterization of pure dECMT after solubilization:
A. Amplitude Sweep of dECMT which has a storage modulus of 46.11Pa in the linear viscoelastic region B. Viscosity curve showing shear thinning behavior. C. Time sweep of dECMT after an immediate change from 4°C to 37°C. D. Temperature ramp from 4°C to 37°C to observe the change in moduli while gelation temperature ramp: 0.2°C/min. E. SEM images of dECMT. F. AFM microscopy of dECMT

4.3.Biochemical Characterization

To determine the biochemical composition of the dECM hydrogel the total protein in the sample was quantified using Bradford Assay. According to the BSA standard in the plot of Figure 6A, the dECMT contains 106±27 µg/ml of protein. To determine precisely which structural proteins remained after the decellularization and solubilization process we did a protein analysis using LC-MS-MS. Since the dECMT was partially digested with the pepsin used for tissue solubilization, the quantification was done by searching semi-tryptic peptides. In Figure 6B we show the list of structural proteins found in the sample in descending order according to the amount of semi-tryptic peptides found. To corroborate the integrity of the three chains of collagen I, we performed an SDS-PAGE using a control of commercially available Collagen I derived from porcine sources.

As seen in Figure 6C, our dECM sample and the collagen control share the α1, α2, β chains confirming the presence of the molecule. Additional protein bands are perceptible in the dECM.

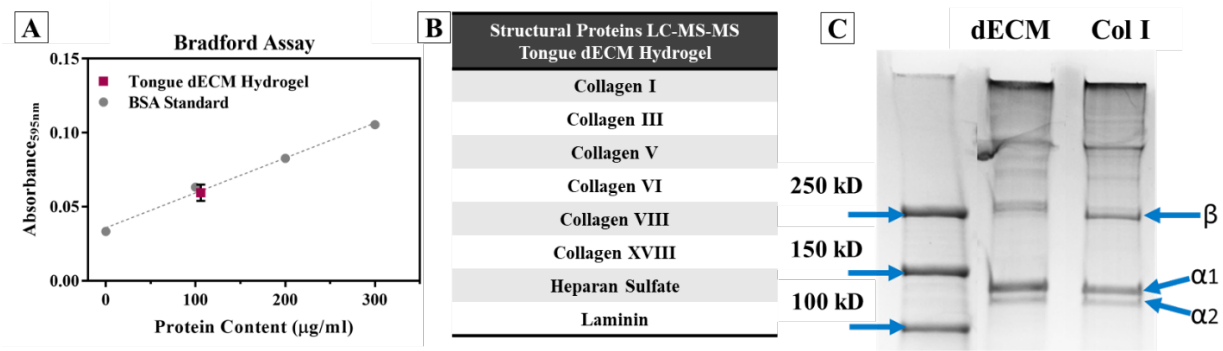

Figure 6- Biochemical characterization of dECMT:
A. Bradford Assay of dECMT using BSA as a standard for protein quantification. Error bars represent the standard deviation of the triplicates of the dECMT. B. Results of semi-tryptic peptides found in dECMT LC-MS-MS test in descendent order considering the number of occurrences of peptides that correspond to the specific protein. C. SDS-PAGE of dECMT using collagen I as a control to compare the existing bands in dECM.

4.4.Cell-viability Assays in dECMT

Cell viability assays were performed with dECMT hydrogel discs that were mold-casted in 48-well plates. After 24 hours of 37°C incubation, discs were cultured in agarose coated Petri dishes for up to 22 days. Triple stain on live samples was done using Calcein-AM for live cells, Ethidium Homodimer for dead cells and Hoechst 33342 for DNA. Samples were imaged using confocal microscopy, cells which were homogeneously distributed throughout the disc on day 1 rearranging into a layer of cells shown the cross-sectional planes of Figure 7. Maximum intensity projection of the acquisition is shown in Figure 8 for both cell lines UM-SCC-12 and UM-SCC-38 formation

of sheet-like structures is observed from day 10. Cells stained in red/purple are observed on day 1 and day 4. However, after day 10 most of the cells captured are viable for the Calcein-AM stain. This assay shows the ability to culture UM-SCC cell lines in the dECMT for up to 22 days with an increase in population and viability over time.

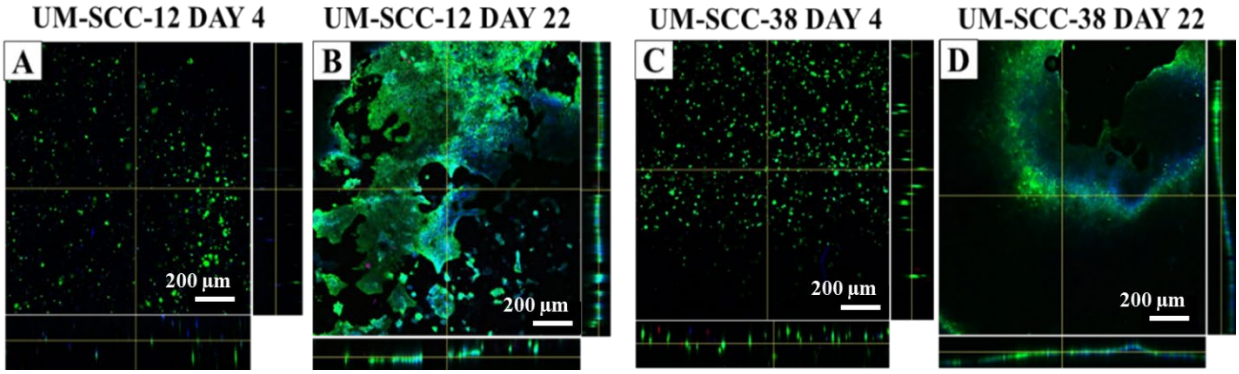

Figure 7- Cross-sectional planes of Confocal Microscopy from Cell Viability Assays in dECMT. Orthogonal views are presented to clearly observe the layer of cells present at day 22 in the yz view (right panel) and xz (bottom panel). The xy and xz panels show the presence of cells in the specific sections shown by the yellow lines in the main image (xy view).

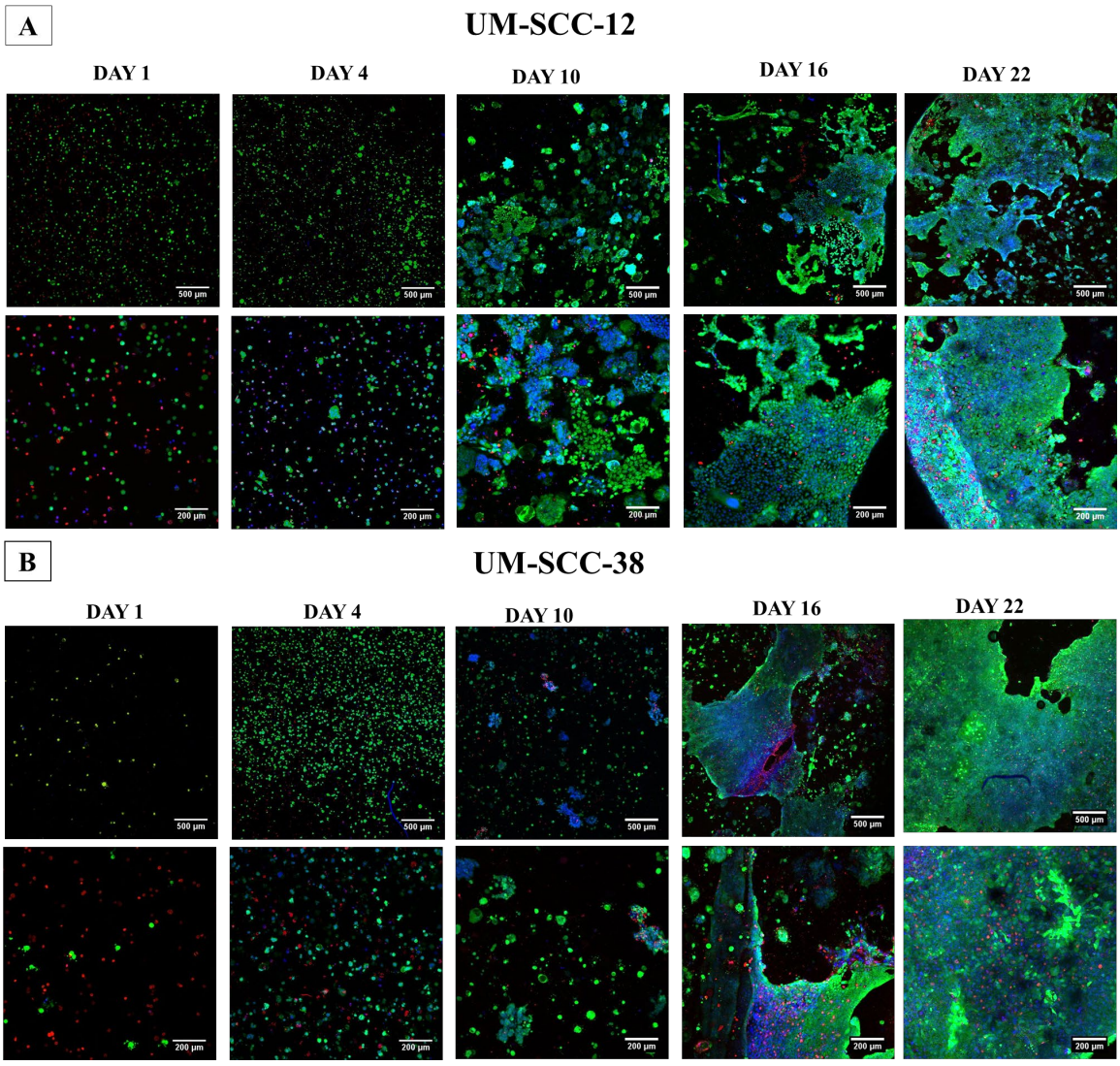

Figure 8- Live-Dead Assay Maximum Intensity Projections:
Maximum intensity of each image was obtained and projected throughout all the z-stack of the acquisition to obtain the images presented above. Confocal microscopy over 22 days mold casted 3D culture of A. UM-SCC-12 and B. UM-SCC-38 cell lines. Red: Ethidium homodimer (dead cells), Green: Calcein-AM (live cells), Hoechst 33342 (DNA). The two images presented at each day correspond to the same sample acquired at different magnifications.

4.5.Histology

For the histology analysis, slides were analyzed blindly by a pathologist. Figure 1 shows the differences between day 1 and day 10 by the formation of cell nests and epithelium forming a coat

in the periphery of the discs which is characteristic of epithelial cells and squamous cell carcinoma. In the last day, the cell periphery grows for up to six layers of cells becoming more continuous than on day 10. We expect the light pink structures shown by the red arrows in Figure 9C and Figure 9F to be early keratin formation; a specific stain is required to confirm.

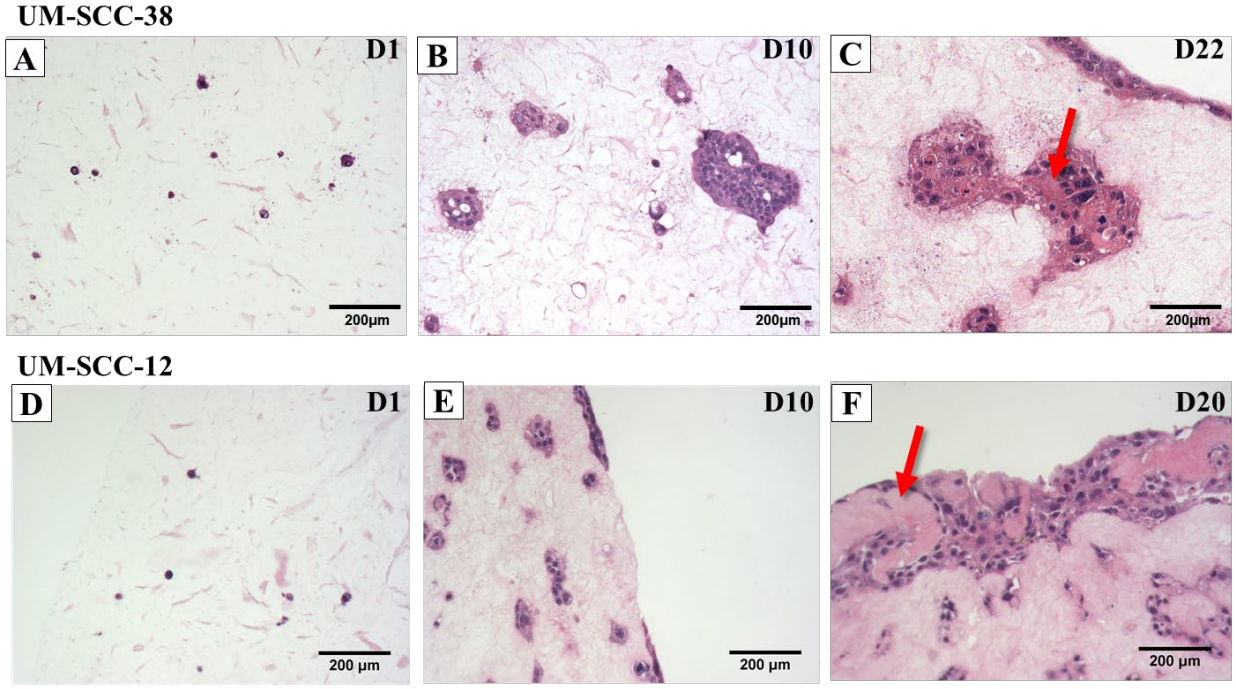

Figure 9- Histology Analysis of Long-Term Culture Assay in dECMT. A-C correspond to UM-SCC-38 and D-F corresponds to UM-SCC-12. Red arrows highlight the light pink stain expected to be keratin formation.

4.6.Printability Assays

The first option was to bioprint pure dECMT. Grid-like structures were successfully achieved for up to two layers. Fabricated structures did not keep their shape, and dECMT started to flow immediately after printing (Figure 10). To create a bioink capable of printing several layers without flowing, we created several blends of dECMT and Carbopol® ETD 2020NF (Table 4). Carbopol® ETD 2020NF is a commercially available blend of carbomer copolymers that contain a block copolymer of polyethylene glycol and a long chain alkyl acid ester. After doing amplitude sweep

tests in all the blends (Figure 11) and quantifying the complex modulus of the material and determining the yield point, we decided to print the blend containing 1% Carbopol® ETD 2020NF (Figure 12A-C). We fabricated grid-like squared structures of 15 layers; the bioink kept its shape without apparent flow after printing (Figure 12F-G). The fabricated structure was immersed in media and incubated at 37°C for 24h (Figure 12D-E). After 12 days in culture media, the Carbopol® ETD 2020NF was dissolved for instance this blend is useful for short-term experiments. Crosslinking of the material may be needed to ensure Carbopol® ETD 2020NF and dECM stability over long periods of time. For this project, no further characterization of the dECMT-Carbopol® ETD 2020NF blend was done, but the calculation of the rate of dissolution, change in mass, and cell viability assay using this blend are considered for future work.

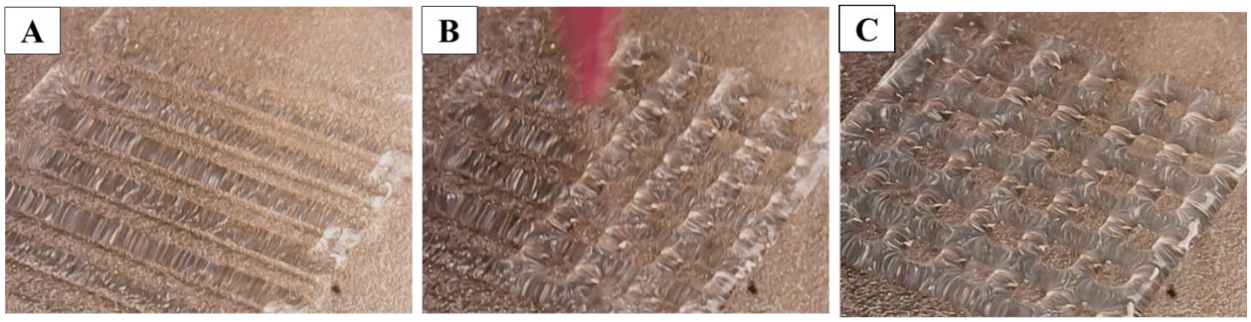

Figure 10-Bioprinting test of pure dECMT hydrogel.

Table 4- dECM-Carbopol® ETD 2020NF Concentrations

Blend	Ratio	Final Carbopol Concentration (wt%)
dECMT+ Carbopol® ETD 2020NF 1% wt	1:1	0.5%
dECMT+ Carbopol® ETD 2020NF 3% wt	2:1	1%
dECMT+ Carbopol® ETD 2020NF 5% wt	2:1	1.67%

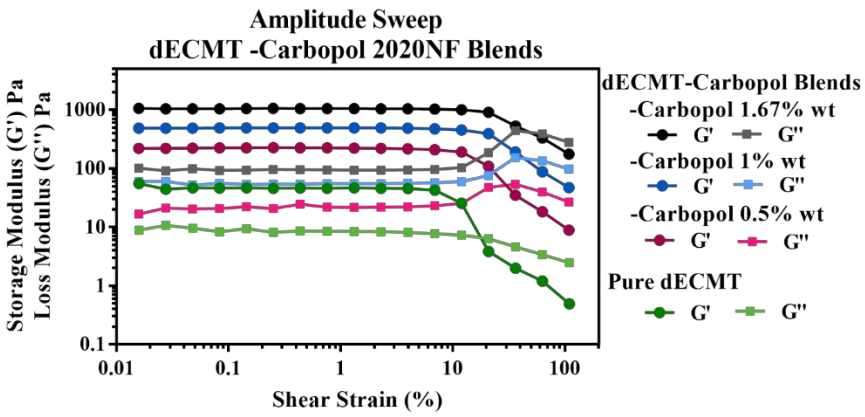

Figure 11- Amplitude Sweep of dECMT-Carbopol® ETD 2020NF Blends:
Amplitude sweeps of blends in Table 4 are shown in this figure. Pure dECMT is displayed as a reference and has the lowest G', G'' compared to all the Carbopol® ETD 2020NF blends. The 1%wt Carbopol® ETD 2020NF blend was chosen to bioprint since the G' is below a 1000Pa. The lower the G', the lower the shear when the material is extruded through the bioprinter tip. If the shearing is too strong, encapsulated cells may be disrupted and viability compromised.

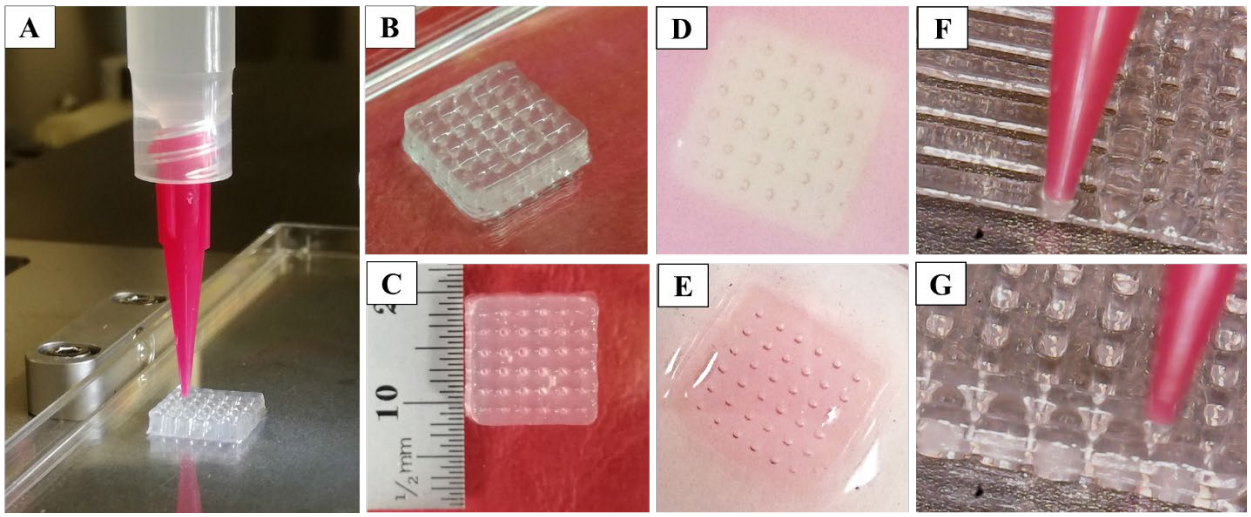

Figure 12- dECMT- Carbopol® ETD 2020NF (1% wt) Bioprinting.
A. Bioprinting dECMT-Carbopol® ETD 2020NF (1% wt) using a G25 tip. B-C. Final structure with 15 layers and 10mm x10mm of width and depth. D. Structure immersed in culture media. E. Structure after 24 hours in culture media at 37°C. F-G. High magnification images of the printing process.

5. DISCUSSION

In this project we developed a biomaterial derived from decellularized porcine tongue and Carbopol® ETD 2020NF. It can be used as a bioink for 3D extrusion printing and serve as a tool to fabricate complex heterogeneous *in vitro* cancer models, specifically to understand the development and treatment of HNSCC. We have successfully decellularized the porcine tongue, removing excess of detergents was a crucial step to promote cell viability in the material. High concentrations of SDS in the decellularized matrix disrupt cell membranes causing death. Commonly used protocols to remove SDS for protein purification incorporate acetone washes [105]. We adapted this method to remove the anionic detergent in our sample which resulted in a dECMT able to sustain cell viability for up to 22 days.

dECMT showed a shear-thinning behavior in the rheological characterization which has been previously observed [102] as well as temperature sensitivity and increase in storage modulus at 37°C. This moduli change also happens in other naturally derived materials such as Matrigel® and Collagen I and has been reported by other groups that decellularized and solubilized tissue [92, 94, 102, 103]. It can be attributed to the thermal crosslinking process caused by the rearrangement and restructuring of proteins including collagen fibers that can reform triple helix structures at physiological temperature [11, 107] making the dECMT insoluble in media. This temperature sensitivity becomes useful to embed cells between 4°C -20°C while the storage modulus and the loss modulus are closer between each other and keep them in the culture at 37°C when thermal gelation occurs.

The presence of collagen in dECMT can be confirmed with the AFM microscopy that clearly shows the ≈67nm distance between one fiber and the other [108]. This bands have been widely reported in in fibrous helix-forming collagens (I, II, III, and V) and is an indicator of the structural

integrity of the molecule [108]. Collagen peptides were also detected by the LC-MS-MS quantification considering collagen I and III were the most abundant proteins after solubilization and are also one of the most abundant proteins in tissues [107]. Our results agree with other studies that have quantified proteins in dECM tissue and found collagen as the most abundant protein [109].

We demonstrated that UM-SCC-12 and UM-SCC-38 remain viable when encapsulated in dECMT and cultured for more than 20 days. We also observed a cell rearrangement into sheets which is a behavior observed in some squamous cell carcinoma cell lines. Only certain tumor cells have spheroid growth capability [110]. Disc contraction was detected and can be attributed to the traction forces exerted by the cells into the fibrous components of the extracellular matrix, many cells such as fibroblasts, smooth muscle cells, and cancer cells exhibit this behavior [106]. It is believed there is a strong association between cell invasion and the traction forces exerted by the cells on the TME [111].

Histology analysis shows cell nest formation by day 10 and possible keratinization by day 22. Keratinising SCC malignancy classification is determined by the amount of keratinization observed, the presence of keratin pearls is associated with a poorly differentiated tumor which does not resemble to normal tissue [112]. Pathological analysis concludes that a moderately to poorly differentiated behavior is observed in dECMT cultured cells.

Pure dECMT printing attempts corroborated the yield point of the material is too low so it is unable to widthstand its own weight resulting in flow and merging of the grid like structure; that happened presumably for the low moduli, and the lack of time for the material to recover after shearing. Only two layers of material were achieved with this bioink. The main cause of this structural weakness is the decellularization and solubilization processes. Using detergents and enzymes partially

disrupts the structural proteins resulting in a weaker material than the original tissue. On the other hand, dECMT-Carbopol® ETD 2020NF 1% blend resulted in a stable bioink able to print grid-like structures of up to 15 layers which maintained their shape after 24 hours in culture conditions and gave enough time for dECM to gel without losing its shape. Carbopol® ETD 2020NF served as a stable reinforcement by increasing the modulus and the yield point of the material while being inert, biocompatible and safe for human consumption. Additional investigation should be done to understand the interaction of dECMT-Carbopol® ETD 2020NF and UM-SCC cell lines considering a crosslinking agent for long-term culture since the blend does not support more than 1 week of physiological conditions. However, our current observations place tongue derived dECM as a potential material to develop bioprinted *in vitro* models for its bioactive components and resemblance to actual ECM.

6. CONCLUSIONS

The compelling need of representative disease models has been pushing the boundaries of tissue engineering in finding an alternative approach to understand and treat malignancies. Improvements in the bioengineering field have made possible the development of complex 3D culture systems as research platforms with the help of 3D bioprinting techniques. More complex materials, such as dECM, have gained interest for their bioactivity and similar characteristics found in the ECM *in vivo*. Using dECMs as bioinks to bioprint heterogeneous cancer models can contribute in filling the gap between overly simple models such as 2D culture monolayers and animal models which have variables difficult to control. Having this midpoint available can give reasearchers significant insights of tumor development and progresson in a more complex but controlled scenario. We face several challenges when using dECM such as mechanical instability but as seen in this project, reinforcement is possible to achieve a stable biomaterial. The goal of

this study was to show that the dECMT-Carbopol® ETD 2020NF blend can be used as a bioink to develop SCC *in vitro* models. We demonstrated dECMT's ability to encapsulate cells and its printability when combined with Carbopol® ETD 2020NF. Further research needs to be done but we believe this technology has a lot of potential not just for HNSCC since it can be adapted to study other neoplasms and diseases resulting in clinically relevant data that will potentially improve the treatment and prognosis of patients and better understanding of biology.

7. FUTURE WORK

To continue with the development of the bioink and the 3D bioprinted model our future work will be focused on tuning the material's characteristics to widthstand long-term culture conditions as well as performing cell viability assays with HNSCC cells embedded in the dECM-Carbopol® ETD 2020NF blend. Also, to study the matrix development over time, proteomic analysis and mechanical testing are considered. In later stages of the project, we will incorporate chemotherapy and radiotherapy treatments into the 3D models to determine tumour resistance and compare our tools's response to small animal models and what has been observed in clinical studies of HNSCC.

8. REFERENCES

[1] World Health Organization, "The global burden of disease: 2004 update. 2008," ed, 2011.

[2] Canadian Cancer Society's Advisory Committee on Cancer Statistics, "Canadian Cancer Statistics 2016," *Canadian Cancer Society, ,* 2016.

[3] E. C. Ward and C. J. van As-Brooks, *Head and neck cancer: treatment, rehabilitation, and outcomes*. Plural Publishing, 2014.

[4] T. J. Keane *et al.*, "Restoring mucosal barrier function and modifying macrophage phenotype with an extracellular matrix hydrogel: potential therapy for ulcerative colitis," *Journal of Crohn's and Colitis,* vol. 11, no. 3, pp. 360-368, 2017.

[5] K.-M. Park *et al.*, "Decellularized liver extracellular matrix as promising tools for transplantable bioengineered liver promotes hepatic lineage commitments of induced pluripotent stem cells," *Tissue Engineering Part A,* vol. 22, no. 5-6, pp. 449-460, 2016.

[6] S. P. Pilipchuk, M. K. Vaicik, J. C. Larson, E. Gazyakan, M.-H. Cheng, and E. M. Brey, "Influence of crosslinking on the stiffness and degradation of dermis-derived hydrogels," *Journal of Biomedical Materials Research Part A,* vol. 101, no. 10, pp. 2883-2895, 2013.

[7] T. J. Keane, I. T. Swinehart, and S. F. Badylak, "Methods of tissue decellularization used for preparation of biologic scaffolds and in vivo relevance," (in eng), *Methods,* vol. 84, pp. 25-34, Aug 2015.

[8] R. Londono and S. F. Badylak, "Biologic scaffolds for regenerative medicine: mechanisms of in vivo remodeling," (in eng), *Ann Biomed Eng,* vol. 43, no. 3, pp. 577-92, Mar 2015.

[9] J. L. Dziki, D. S. Wang, C. Pineda, B. M. Sicari, T. Rausch, and S. F. Badylak, "Solubilized extracellular matrix bioscaffolds derived from diverse source tissues differentially influence macrophage phenotype," (in eng), *J Biomed Mater Res A,* vol. 105, no. 1, pp. 138-147, Jan 2017.

[10] T. J. Keane *et al.*, "Preparation and characterization of a biologic scaffold and hydrogel derived from colonic mucosa," (in eng), *J Biomed Mater Res B Appl Biomater,* vol. 105, no. 2, pp. 291-306, Feb 2017.

[11] L. T. Saldin, M. C. Cramer, S. S. Velankar, L. J. White, and S. F. Badylak, "Extracellular matrix hydrogels from decellularized tissues: Structure and function," (in eng), *Acta Biomater,* vol. 49, pp. 1-15, Feb 2017.

[12] G. M. Cooper and R. E. Hausman, *The Cell: A Molecular Approach*. Sinauer Associates, 2013.

[13] N. Denaro, E. G. Russi, V. Adamo, and M. C. Merlano, "State-of-the-art and emerging treatment options in the management of head and neck cancer: news from 2013," *Oncology,* vol. 86, no. 4, pp. 212-229, 2014.

[14] A. E. Albers, L. Strauss, T. Liao, T. Hoffmann, and A. Kaufmann, "T cell-tumor interaction directs the development of immunotherapies in head and neck cancer," *Clinical and Developmental Immunology,* vol. 2010, 2010.

[15] W. J. Blot *et al.*, "Smoking and drinking in relation to oral and pharyngeal cancer," *Cancer research,* vol. 48, no. 11, pp. 3282-3287, 1988.

[16] S. Franceschi, E. Bidoli, R. Herrero, and N. Munoz, "Comparison of cancers of the oral cavity and pharynx worldwide: etiological clues," *Oral oncology,* vol. 36, no. 1, pp. 106-115, 2000.

[17] A. Auluck, G. Hislop, C. Bajdik, C. Poh, L. Zhang, and M. Rosin, "Trends in oropharyngeal and oral cavity cancer incidence of human papillomavirus (HPV)-related and HPV-unrelated sites in a multicultural population: the British Columbia experience," *Cancer: Interdisciplinary International Journal of the American Cancer Society,* vol. 116, no. 11, pp. 2635-2644, 2010.

[18] A. K. Chaturvedi, E. A. Engels, W. F. Anderson, and M. L. Gillison, "Incidence trends for human papillomavirus-related and-unrelated oral squamous cell carcinomas in the United States," *Journal of clinical oncology,* vol. 26, no. 4, pp. 612-619, 2008.

[19] D. Conway, D. Stockton, K. Warnakulasuriya, G. Ogden, and L. Macpherson, "Incidence of oral and oropharyngeal cancer in United Kingdom (1990–1999)—recent trends and regional variation," *Oral oncology,* vol. 42, no. 6, pp. 586-592, 2006.

[20] R. Siegel, D. Naishadham, and A. Jemal, "Cancer statistics, 2013," *CA: a cancer journal for clinicians,* vol. 63, no. 1, pp. 11-30, 2013.

[21] J.-P. Pignon, A. Le Maitre, E. Maillard, J. Bourhis, and M.-N. C. Group, "Meta-analysis of chemotherapy in head and neck cancer (MACH-NC): an update on 93 randomised trials and 17,346 patients," *Radiotherapy and Oncology,* vol. 92, no. 1, pp. 4-14, 2009.

[22] B. E. Brockstein, "Management of Recurrent Head and Neck Cancer," *Drugs,* vol. 71, no. 12, pp. 1551-1559, 2011.

[23] F. R. Balkwill, M. Capasso, and T. Hagemann, "The tumor microenvironment at a glance," ed: The Company of Biologists Ltd, 2012.

[24] B.-Z. Qian and J. W. Pollard, "Macrophage diversity enhances tumor progression and metastasis," *Cell,* vol. 141, no. 1, pp. 39-51, 2010.

[25] M. S. Samuel *et al.*, "Actomyosin-mediated cellular tension drives increased tissue stiffness and β-catenin activation to induce epidermal hyperplasia and tumor growth," *Cancer cell,* vol. 19, no. 6, pp. 776-791, 2011.

[26] P. Lu, V. M. Weaver, and Z. Werb, "The extracellular matrix: A dynamic niche in cancer progression," *The Journal of Cell Biology,* vol. 196, no. 4, pp. 395-406, 2012.

[27] C. Frantz, K. M. Stewart, and V. M. Weaver, "The extracellular matrix at a glance," *J Cell Sci,* vol. 123, no. 24, pp. 4195-4200, 2010.

[28] J. A. Joyce and J. W. Pollard, "Microenvironmental regulation of metastasis," *Nature Reviews Cancer,* vol. 9, no. 4, p. 239, 2009.

[29] F. Pampaloni, E. G. Reynaud, and E. H. Stelzer, "The third dimension bridges the gap between cell culture and live tissue," *Nature reviews Molecular cell biology,* vol. 8, no. 10, p. 839, 2007.

[30] M. W. Taylor, "A history of cell culture," in *Viruses and man: a history of interactions*: Springer, 2014, pp. 41-52.

[31] K. M. Yamada and E. Cukierman, "Modeling tissue morphogenesis and cancer in 3D," *Cell,* vol. 130, no. 4, pp. 601-610, 2007.

[32] A. Birgersdotter, R. Sandberg, and I. Ernberg, "Gene expression perturbation in vitro—a growing case for three-dimensional (3D) culture systems," in *Seminars in cancer biology*, 2005, vol. 15, no. 5, pp. 405-412: Elsevier.

[33] B. A. Ruggeri, F. Camp, and S. Miknyoczki, "Animal models of disease: pre-clinical animal models of cancer and their applications and utility in drug discovery," *Biochemical pharmacology,* vol. 87, no. 1, pp. 150-161, 2014.

[34] M. Hay, D. W. Thomas, J. L. Craighead, C. Economides, and J. Rosenthal, "Clinical development success rates for investigational drugs," *Nature biotechnology,* vol. 32, no. 1, p. 40, 2014.

[35] A. Nyga, U. Cheema, and M. Loizidou, "3D tumour models: novel in vitro approaches to cancer studies," *Journal of cell communication and signaling,* vol. 5, no. 3, p. 239, 2011.

[36] B. A. Ruggeri, F. Camp, and S. Miknyoczki, "Animal models of disease: pre-clinical animal models of cancer and their applications and utility in drug discovery," (in Eng), *Biochem Pharmacol,* vol. 87, no. 1, pp. 150-61, Jan 1 2014.

[37] D. W. McMillin, J. M. Negri, and C. S. Mitsiades, "The role of tumour–stromal interactions in modifying drug response: challenges and opportunities," *Nature Reviews Drug Discovery,* Review Article vol. 12, p. 217, 03/01/online 2013.

[38] M. Bibby, "Orthotopic models of cancer for preclinical drug evaluation: advantages and disadvantages," *European journal of cancer,* vol. 40, no. 6, pp. 852-857, 2004.

[39] M. Singh and L. Johnson, "Using genetically engineered mouse models of cancer to aid drug development: an industry perspective," *Clinical Cancer Research,* vol. 12, no. 18, pp. 5312-5328, 2006.

[40] A. L. Kung, "Practices and pitfalls of mouse cancer models in drug discovery," *Advances in cancer research,* vol. 96, pp. 191-212, 2006.

[41] Y. S. DeRose *et al.*, "Tumor grafts derived from women with breast cancer authentically reflect tumor pathology, growth, metastasis and disease outcomes," *Nature medicine,* vol. 17, no. 11, p. 1514, 2011.

[42] M. Hidalgo *et al.*, "A pilot clinical study of treatment guided by personalized tumorgrafts in patients with advanced cancer," *Molecular cancer therapeutics,* p. molcanther. 0233.2011, 2011.

[43] S. Banerjee, S. Manna, P. Saha, C. K. Panda, and S. Das, "Black tea polyphenols suppress cell proliferation and induce apoptosis during benzo (a) pyrene-induced lung carcinogenesis," *European Journal of Cancer Prevention,* vol. 14, no. 3, pp. 215-221, 2005.

[44] E. L. Abel, J. M. Angel, K. Kiguchi, and J. DiGiovanni, "Multi-stage chemical carcinogenesis in mouse skin: fundamentals and applications," *Nature protocols,* vol. 4, no. 9, p. 1350, 2009.

[45] D. E. Bassi and A. Klein-Szanto, "Carcinogen-Induced Animal Models of Head and Neck Squamous Cell Carcinoma," *Current protocols in pharmacology,* vol. 37, no. 1, pp. 14.2. 1-14.2. 19, 2007.

[46] S. I. Grivennikov, F. R. Greten, and M. Karin, "Immunity, inflammation, and cancer," *Cell,* vol. 140, no. 6, pp. 883-899, 2010.

[47] I. E. Holopainen, "Organotypic hippocampal slice cultures: a model system to study basic cellular and molecular mechanisms of neuronal cell death, neuroprotection, and synaptic plasticity," *Neurochemical research,* vol. 30, no. 12, pp. 1521-1528, 2005.

[48] J. M. Kelm, N. E. Timmins, C. J. Brown, M. Fussenegger, and L. K. Nielsen, "Method for generation of homogeneous multicellular tumor spheroids applicable to a wide variety of cell types," *Biotechnology and bioengineering,* vol. 83, no. 2, pp. 173-180, 2003.

[49] F. Castañeda and R. K. Kinne, "Short exposure to millimolar concentrations of ethanol induces apoptotic cell death in multicellular HepG2 spheroids," *Journal of cancer research and clinical oncology,* vol. 126, no. 6, pp. 305-310, 2000.

[50] R. Barbucci, *Hydrogels: Biological properties and applications*. Springer Science & Business Media, 2010.

[51] S. J. Bryant and K. S. Anseth, "Hydrogel properties influence ECM production by chondrocytes photoencapsulated in poly (ethylene glycol) hydrogels," *Journal of Biomedical Materials Research: An Official Journal of The Society for Biomaterials and The Japanese Society for Biomaterials,* vol. 59, no. 1, pp. 63-72, 2002.

[52] L. Hockaday *et al.*, "Rapid 3D printing of anatomically accurate and mechanically heterogeneous aortic valve hydrogel scaffolds," *Biofabrication,* vol. 4, no. 3, p. 035005, 2012.

[53] C. N. Salinas and K. S. Anseth, "The influence of the RGD peptide motif and its contextual presentation in PEG gels on human mesenchymal stem cell viability," *Journal of tissue engineering and regenerative medicine,* vol. 2, no. 5, pp. 296-304, 2008.

[54] M. W. Tibbitt and K. S. Anseth, "Hydrogels as extracellular matrix mimics for 3D cell culture," *Biotechnology and Bioengineering,* vol. 103, no. 4, pp. 655-663, 2009.

[55] B. Duan, L. A. Hockaday, K. H. Kang, and J. T. Butcher, "3D bioprinting of heterogeneous aortic valve conduits with alginate/gelatin hydrogels," *Journal of biomedical materials research Part A,* vol. 101, no. 5, pp. 1255-1264, 2013.

[56] X. Cui and T. Boland, "Human microvasculature fabrication using thermal inkjet printing technology," *Biomaterials,* vol. 30, no. 31, pp. 6221-6227, 2009.

[57] P. A. Janmey, J. P. Winer, and J. W. Weisel, "Fibrin gels and their clinical and bioengineering applications," *Journal of the Royal Society Interface,* vol. 6, no. 30, pp. 1-10, 2009.

[58] M. N. Nakatsu *et al.*, "Angiogenic sprouting and capillary lumen formation modeled by human umbilical vein endothelial cells (HUVEC) in fibrin gels: the role of fibroblasts and Angiopoietin-1☆," *Microvascular research,* vol. 66, no. 2, pp. 102-112, 2003.

[59] M. Hospodiuk, M. Dey, D. Sosnoski, and I. T. Ozbolat, "The bioink: a comprehensive review on bioprintable materials," *Biotechnology advances,* vol. 35, no. 2, pp. 217-239, 2017.

[60] S. Zhong, D. Campoccia, P. Doherty, R. Williams, L. Benedetti, and D. Williams, "Biodegradation of hyaluronic acid derivatives by hyaluronidase," *Biomaterials,* vol. 15, no. 5, pp. 359-365, 1994.

[61] B. P. Toole, "Hyaluronan: from extracellular glue to pericellular cue," *Nature Reviews Cancer,* vol. 4, no. 7, p. 528, 2004.

[62] J. A. Burdick and G. D. Prestwich, "Hyaluronic acid hydrogels for biomedical applications," *Advanced materials,* vol. 23, no. 12, pp. H41-H56, 2011.

[63] S. Gerecht, J. A. Burdick, L. S. Ferreira, S. A. Townsend, R. Langer, and G. Vunjak-Novakovic, "Hyaluronic acid hydrogel for controlled self-renewal and differentiation of human embryonic stem cells," *Proceedings of the National Academy of Sciences,* vol. 104, no. 27, pp. 11298-11303, 2007.

[64] L. Pescosolido *et al.*, "Biodegradable IPNs based on oxidized alginate and dextran-HEMA for controlled release of proteins," *Carbohydrate polymers,* vol. 86, no. 1, pp. 208-213, 2011.

[65] A. Skardal, J. Zhang, and G. D. Prestwich, "Bioprinting vessel-like constructs using hyaluronan hydrogels crosslinked with tetrahedral polyethylene glycol tetracrylates," *Biomaterials,* vol. 31, no. 24, pp. 6173-6181, 2010.

[66] M. S. Hahn, B. A. Teply, M. M. Stevens, S. M. Zeitels, and R. Langer, "Collagen composite hydrogels for vocal fold lamina propria restoration," *Biomaterials,* vol. 27, no. 7, pp. 1104-1109, 2006.

[67] T. D. Sargeant, A. P. Desai, S. Banerjee, A. Agawu, and J. B. Stopek, "An in situ forming collagen–PEG hydrogel for tissue regeneration," *Acta biomaterialia,* vol. 8, no. 1, pp. 124-132, 2012.

[68] S. L. Voytik-Harbin, A. O. Brightman, B. Z. Waisner, J. P. Robinson, and C. H. Lamar, "Small intestinal submucosa: a tissue-derived extracellular matrix that promotes tissue-

specific growth and differentiation of cells in vitro," *Tissue engineering,* vol. 4, no. 2, pp. 157-174, 1998.

[69] K. H. Nakayama, C. A. Batchelder, C. I. Lee, and A. F. Tarantal, "Decellularized rhesus monkey kidney as a three-dimensional scaffold for renal tissue engineering," *Tissue Engineering Part A,* vol. 16, no. 7, pp. 2207-2216, 2010.

[70] X. Dong *et al.*, "RGD-modified acellular bovine pericardium as a bioprosthetic scaffold for tissue engineering," *Journal of Materials Science: Materials in Medicine,* vol. 20, no. 11, p. 2327, 2009.

[71] J. Zhou *et al.*, "Impact of heart valve decellularization on 3-D ultrastructure, immunogenicity and thrombogenicity," *Biomaterials,* vol. 31, no. 9, pp. 2549-2554, 2010.

[72] S. B. Lumpkins, N. Pierre, and P. S. McFetridge, "A mechanical evaluation of three decellularization methods in the design of a xenogeneic scaffold for tissue engineering the temporomandibular joint disc," *Acta biomaterialia,* vol. 4, no. 4, pp. 808-816, 2008.

[73] O. Gorschewsky, A. Klakow, K. Riechert, M. Pitzl, and R. Becker, "Clinical comparison of the Tutoplast allograft and autologous patellar tendon (bone-patellar tendon-bone) for the reconstruction of the anterior cruciate ligament: 2-and 6-year results," *The American journal of sports medicine,* vol. 33, no. 8, pp. 1202-1209, 2005.

[74] T. H. Petersen *et al.*, "Tissue-engineered lungs for in vivo implantation," *Science,* p. 1189345, 2010.

[75] I. Tudorache *et al.*, "Tissue engineering of heart valves: biomechanical and morphological properties of decellularized heart valves," *The Journal of heart valve disease,* vol. 16, no. 5, pp. 567-73; discussion 574, 2007.

[76] I. Prasertsung, S. Kanokpanont, T. Bunaprasert, V. Thanakit, and S. Damrongsakkul, "Development of acellular dermis from porcine skin using periodic pressurized technique," *Journal of Biomedical Materials Research Part B: Applied Biomaterials: An Official Journal of The Society for Biomaterials, The Japanese Society for Biomaterials, and The Australian Society for Biomaterials and the Korean Society for Biomaterials,* vol. 85, no. 1, pp. 210-219, 2008.

[77] R.-N. Chen, H.-O. Ho, Y.-T. Tsai, and M.-T. Sheu, "Process development of an acellular dermal matrix (ADM) for biomedical applications," *Biomaterials,* vol. 25, no. 13, pp. 2679-2686, 2004.

[78] B. D. Elder, D. H. Kim, and K. A. Athanasiou, "Developing an articular cartilage decellularization process toward facet joint cartilage replacement," *Neurosurgery,* vol. 66, no. 4, pp. 722-727, 2010.

[79] L. Flynn, "The use of decellularized adipose tissue to provide an inductive microenvironment for the adipogenic differentiation of human adipose-derived stem cells," *Biomaterials,* vol. 31, no. 17, pp. 4715-4724, 2010.

[80] M.-T. Kasimir *et al.*, "Comparison of different decellularization procedures of porcine heart valves," *The International journal of artificial organs,* vol. 26, no. 5, pp. 421-427, 2003.

[81] M. Paulsson, "Basement membrane proteins: structure, assembly, and cellular interactions," *Critical reviews in biochemistry and molecular biology,* vol. 27, no. 1-2, pp. 93-127, 1992.

[82] G. Benton, I. Arnaoutova, J. George, H. K. Kleinman, and J. Koblinski, "Matrigel: from discovery and ECM mimicry to assays and models for cancer research," *Advanced drug delivery reviews,* vol. 79, pp. 3-18, 2014.

[83] R. Elliot Jr, "Use of commercial procine skin for wound dressing," *Plast. Reconstr. Surg.,* vol. 52, pp. 401-405, 1973.

[84] P. M. Crapo, T. W. Gilbert, and S. F. Badylak, "An overview of tissue and whole organ decellularization processes," *Biomaterials,* vol. 32, no. 12, pp. 3233-3243, 2011/04/01/ 2011.

[85] H. C. Ott *et al.*, "Perfusion-decellularized matrix: using nature's platform to engineer a bioartificial heart," *Nature medicine,* vol. 14, no. 2, p. 213, 2008.

[86] T. Shupe, M. Williams, A. Brown, B. Willenberg, and B. E. Petersen, "Method for the decellularization of intact rat liver," *Organogenesis,* vol. 6, no. 2, pp. 134-136, 2010.

[87] E. A. Ross *et al.*, "Embryonic stem cells proliferate and differentiate when seeded into kidney scaffolds," *Journal of the American Society of Nephrology,* vol. 20, no. 11, pp. 2338-2347, 2009.

[88] Y. Kubota, H. K. Kleinman, G. R. Martin, and T. J. Lawley, "Role of laminin and basement membrane in the morphological differentiation of human endothelial cells into capillary-like structures," *The Journal of cell biology,* vol. 107, no. 4, pp. 1589-1598, 1988.

[89] T. K. Feaster *et al.*, "Matrigel mattress: a method for the generation of single contracting human-induced pluripotent stem cell–derived cardiomyocytes," *Circulation research,* vol. 117, no. 12, pp. 995-1000, 2015.

[90] G. Benton, J. George, H. Kleinman, and I. Arnaoutova, "Advancing science and technology via 3D culture on basement membrane matrix," *Journal of cellular physiology,* vol. 221, no. 1, pp. 18-25, 2009.

[91] S. Vukicevic, H. K. Kleinman, F. P. Luyten, A. B. Roberts, N. S. Roche, and A. Reddi, "Identification of multiple active growth factors in basement membrane Matrigel suggests caution in interpretation of cellular activity related to extracellular matrix components," *Experimental cell research,* vol. 202, no. 1, pp. 1-8, 1992.

[92] D. O. Freytes, J. Martin, S. S. Velankar, A. S. Lee, and S. F. Badylak, "Preparation and rheological characterization of a gel form of the porcine urinary bladder matrix," (in Eng), *Biomaterials,* vol. 29, no. 11, pp. 1630-7, Apr 2008.

[93] S. Uriel *et al.*, "The role of adipose protein derived hydrogels in adipogenesis," *Biomaterials,* vol. 29, no. 27, pp. 3712-3719, 2008.

[94] D. J. S. Hulmes, "Collagen Diversity, Synthesis and Assembly," in *Collagen: Structure and Mechanics*, P. Fratzl, Ed. Boston, MA: Springer US, 2008, pp. 15-47.

[95] Y. Fu *et al.*, "Decellularization of porcine skeletal muscle extracellular matrix for the formulation of a matrix hydrogel: a preliminary study," *Journal of cellular and molecular medicine,* vol. 20, no. 4, pp. 740-749, 2016.

[96] M. Ahearne and A. P. Lynch, "Early observation of extracellular matrix-derived hydrogels for corneal stroma regeneration," *Tissue Engineering Part C: Methods,* vol. 21, no. 10, pp. 1059-1069, 2015.

[97] J. Wu *et al.*, "An injectable extracellular matrix derived hydrogel for meniscus repair and regeneration," *Acta biomaterialia,* vol. 16, pp. 49-59, 2015.

[98] L. W. Dunne *et al.*, "Human decellularized adipose tissue scaffold as a model for breast cancer cell growth and drug treatments," *Biomaterials,* vol. 35, no. 18, pp. 4940-4949, 2014.

[99] P. VODIČKA *et al.*, "The miniature pig as an animal model in biomedical research," *Annals of the New York Academy of Sciences,* vol. 1049, no. 1, pp. 161-171, 2005.

[100] V. Mironov, R. P. Visconti, V. Kasyanov, G. Forgacs, C. J. Drake, and R. R. Markwald, "Organ printing: tissue spheroids as building blocks," *Biomaterials,* vol. 30, no. 12, pp. 2164-2174, 2009.

[101] T. Jiang *et al.*, "Directing the self-assembly of tumour spheroids by bioprinting cellular heterogeneous models within alginate/gelatin hydrogels," *Scientific Reports,* vol. 7, no. 1, p. 4575, 2017.

[102] F. Pati *et al.*, "Printing three-dimensional tissue analogues with decellularized extracellular matrix bioink," (in Eng), *Nat Commun,* vol. 5, p. 3935, Jun 02 2014.

[103] J. Jang, T. G. Kim, B. S. Kim, S.-W. Kim, S.-M. Kwon, and D.-W. Cho, "Tailoring mechanical properties of decellularized extracellular matrix bioink by vitamin B2-induced photo-crosslinking," *Acta biomaterialia,* vol. 33, pp. 88-95, 2016.

[104] Lubrizol Advanced Materials Inc. (2018). *Pharmaceutical Literature*. Available: https://www.lubrizol.com/Life-Sciences/Literature/Pharmaceutical-Literature

[105] P. Matsudaira and P. T. Matsudaira, *A practical guide to protein and peptide purification for microsequencing*. Gulf Professional Publishing, 1993.

[106] K. S. Kopanska, M. Bussonnier, S. Geraldo, A. Simon, D. Vignjevic, and T. Betz, "Chapter 19 - Quantification of collagen contraction in three-dimensional cell culture," in *Methods in Cell Biology*, vol. 125, E. K. Paluch, Ed.: Academic Press, 2015, pp. 353-372.

[107] D. Hulmes, "Collagen diversity, synthesis and assembly," in *Collagen*: Springer, 2008, pp. 15-47.

[108] H. Lodish, A. Berk, S. L. Zipursky, P. Matsudaira, D. Baltimore, and J. Darnell, *Molecular cell biology*. WH Freeman New York, 1995.

[109] J. A. DeQuach *et al.*, "Simple and High Yielding Method for Preparing Tissue Specific Extracellular Matrix Coatings for Cell Culture," *PLOS ONE,* vol. 5, no. 9, p. e13039, 2010.

[110] B. Méry *et al.*, "Preclinical models in HNSCC: A comprehensive review," *Oral oncology,* vol. 65, pp. 51-56, 2017.

[111] T. M. Koch, S. Münster, N. Bonakdar, J. P. Butler, and B. Fabry, "3D traction forces in cancer cell invasion," *PloS one,* vol. 7, no. 3, p. e33476, 2012.

[112] A. Cardesa and P. Slootweg, *Pathology of the Head and Neck*. Springer Berlin Heidelberg, 2006.